Impact of the heterogeneous hydrolysis of N_2O_5 on chemistry and nitrate aerosol formation in the lower troposphere under photosmog conditions

N. Riemer,[1] H. Vogel, and B. Vogel
Institut für Meteorologie und Klimaforschung, Forschungszentrum Karlsruhe/Universität Karlsruhe, Karlsruhe, Germany

B. Schell, I. Ackermann, C. Kessler, and H. Hass
Ford Forschungszentrum Aachen, Aachen, Germany

Received 10 April 2002; revised 18 September 2002; accepted 18 September 2002; published 27 February 2003.

[1] The impact of the heterogeneous hydrolysis of N_2O_5 on tropospheric gas phase and particle phase chemistry was investigated by performing model simulations with two comprehensive model systems and taking into account recent findings on the heterogeneous reaction probability of N_2O_5. Hereby, we focused on photosmog conditions in the lower troposphere. Chemistry box model runs were carried out neglecting transport and deposition processes. The heterogeneous hydrolysis of N_2O_5 leads to a decrease of ozone under low-NO_x conditions and to a strong increase of ozone under high-NO_x conditions. One-dimensional simulations were performed to take into account vertical mixing processes, deposition, and temporal changes of the emissions. The rate constant for the heterogeneous hydrolysis was determined depending on the simulated aerosol surface area density. A large impact of the heterogeneous hydrolysis on the nocturnal concentrations of N_2O_5, NO_3, HNO_3, and the surface area density and nitrate content of the aerosol is found. However, the effect of the hydrolysis of N_2O_5 on ozone decreases considerably compared to the box model simulations. Three-dimensional simulations for a typical summer smog situation for the southwestern part of Germany and on the European scale, which cover a variety of atmospheric and emission conditions, confirm these findings. The impact of heterogeneous hydrolysis on ozone is small, but it causes remarkable changes in the nocturnal concentrations of nitrogen-containing species and on aerosol properties such as surface area density and nitrate content. *INDEX TERMS:* 0305 Atmospheric Composition and Structure: Aerosols and particles (0345, 4801); 0343 Atmospheric Composition and Structure: Planetary atmospheres (5405, 5407, 5409, 5704, 5705, 5707); 0365 Atmospheric Composition and Structure: Troposphere—composition and chemistry; 0368 Atmospheric Composition and Structure: Troposphere—constituent transport and chemistry; *KEYWORDS:* Heterogeneous hydrolysis, tropospheric chemistry, aerosol formation, modelling

Citation: Riemer, N., H. Vogel, B. Vogel, B. Schell, I. Ackermann, C. Kessler, and H. Hass, Impact of the heterogeneous hydrolysis of N_2O_5 on chemistry and nitrate aerosol formation in the lower troposphere under photosmog conditions, *J. Geophys. Res.*, *108*(D4), 4144, doi:10.1029/2002JD002436, 2003.

1. Introduction

[2] Tropospheric chemistry depends critically on the budget of nitrogen oxides (NO_x) [*Ehhalt and Drummond*, 1982]. They control the cycle of odd hydrogen (HO_x) and hence determine the photochemical production of ozone. Their primary sources are emissions of NO_x resulting from fossil fuel combustion processes. Other sources include the natural release of NO_x from soils [*Ludwig et al.*, 2001], biomass burning and lightning [*Logan*, 1983]. The most important removal path for nitrogen from the atmosphere is the formation of HNO_3, which is eventually deposited or scavenged. Since HNO_3 is subject to partitioning between gas phase and particle phase the influence of nitrogen oxides is not limited to gas phase chemistry but also extends to the composition of tropospheric aerosol particles. During daytime the formation of HNO_3 occurs via the reaction of NO_2 and OH. During the night heterogeneous hydrolysis of N_2O_5 on the surface of aqueous aerosol particles represents another possibility for NO_x to be removed from the atmosphere and leads to HNO_3 formation as well [*Platt et al.*, 1984].

[3] The reaction rate of the hydrolysis of N_2O_5 on atmospheric aerosol particles can be quantified by the reaction probability γ_{N2O5}. It has been measured for surfaces of

[1]Now at Department of Mechanical and Aeronautical Engineering, University of California, Davis, Davis, California, USA.

0148-0227/03/2002JD002436$09.00

different aqueous solutions by several techniques [*Mozurkewich and Calvert*, 1988; *Van Doren et al.*, 1990; *Fenter et al.*, 1996, *Robinson et al.*, 1997; *Behnke et al.*, 1997; *Hu and Abbatt*, 1997; *Hallquist et al.*, 2000]. For most solutions typical values for γ_{N2O5} are of the order of 10^{-2}. For solutions, which contain nitrate, however, γ_{N2O5} was found to be one order of magnitude smaller [*Mentel et al.*, 1999].

[4] Several attempts have been made to implement the heterogeneous N_2O_5 hydrolysis in chemical transport models. In the past these models usually did not treat the particle phase explicitly, therefore the heterogeneous loss was often parameterized as a first order reaction as a function of relative humidity. For example, *Chang et al.* [1987] used a first-order rate coefficient based on the measurements by *Platt et al.* [1984], which depended on relative humidity only.

[5] *Hendricks* [1997] investigated the role of heterogeneous reactions on sulfate particles in the tropopause region. He determined a rate constant for the heterogeneous hydrolysis based on a γ_{N2O5} of 0.1 for a monodisperse aerosol population. He compared this rate constant with the parameterization of *Chang et al.* [1987] and found large differences.

[6] *Dentener and Crutzen* [1993] investigated the importance of the heterogeneous hydrolysis of N_2O_5 on the global scale. Their parameterization of the rate constant was based on the aerosol surface area density and on a value for γ_{N2O5} of about 0.1 measured by *Mozurkewich and Calvert* [1988]. They demonstrated that for the northern hemisphere, heterogeneous N_2O_5 hydrolysis affects tropospheric chemistry significantly. However, the aerosol surface area was calculated using a simplified parameterization and nonmethane hydrocarbon chemistry was not included. On the basis of an investigation with a 0-D box model they recommended including the reaction in regional scale models when summer smog episodes are investigated.

[7] In this study we address this aspect in more detail. The impact of the N_2O_5 hydrolysis on tropospheric gas phase and particle phase chemistry is investigated for summer conditions, using recently published values for γ_{N2O5} by *Wahner et al.* [1998] and *Mentel et al.* [1999]. For a systematic analysis we first carried out box model simulations with the RADM2 (Regional Acid Deposition Model; *Stockwell et al.*, [1990]) chemical mechanism to study the interactions based on pure chemistry. Then simulations with a 1-D and a 3-D version of the comprehensive model system KAMM/DRAIS (Karlsruher Atmosphärisches Mesoskaliges Modell/Dreidimensionales Regionales Ausbreitungs-Immissions-Simulationsmodell; *Vogel et al.* [1995]) were performed for the mesoscale. For the 1-D and 3-D simulations, a basis version of the Modal Aerosol Dynamics model for Europe (MADE, *Ackermann et al.* [1998]) was included in the model system KAMM/DRAIS for the explicit treatment of the particle phase. Finally, simulations for the European scale were carried out using the European Air Pollution and Dispersion model (EURAD, *Ebel et al.* [1997]) combined with the full version of MADE [*Ackermann et al.*, 1998; *Schell et al.*, 2001]. While the simulations with KAMM/DRAIS were performed for cloud free conditions for the southwestern part of Germany during summertime, the simulations with EURAD/MADE cover a situation with cloud events for whole western Europe. The different simulations were carried out to cover a broad range of photochemical conditions. We will quantify the impact of the heterogeneous hydrolysis of N_2O_5 on the concentrations of O_3, N_2O_5, NO_3, HNO_3, the aerosol surface area density, and on the nitrate content of the aerosol particles.

2. Parameterization of the Heterogeneous Hydrolysis of N_2O_5

[8] During daytime the most important removal path for NO_x in the atmosphere is the formation of HNO_3 by the reaction of NO_2 and OH.

$$NO_2 + OH \rightarrow HNO_3 \quad \text{(R1)}$$

[9] Reaction R1 also provides an important loss mechanism for OH under polluted conditions. The appearance of NO_3, formed by the reaction of NO_2 and O_3, is characteristic of nighttime chemistry.

$$NO_2 + O_3 \rightarrow NO_3 + O_2 \quad \text{(R2)}$$

NO_3 further reacts with NO_2 to form N_2O_5. Due to rapid photolysis, significant concentrations of NO_3, and hence N_2O_5, can only be reached during the night. N_2O_5 is thermally unstable and decomposes back to NO_2 and NO_3, building up an equilibrium.

$$NO_3 + NO_2 \rightarrow N_2O_5 \quad \text{(R3)}$$

$$N_2O_5 \rightarrow NO_2 + NO_3 \quad \text{(R4)}$$

NO_3 reacts with a number of volatile organic compounds (VOC) such as monoterpenes and phenols and initiates the formation of peroxy and hydroxy radicals [*Platt et al.*, 1990; *Mihelcic et al.*, 1993] and finally organic nitrates and nitric acid.

$$NO_3 + VOC \rightarrow organic\ products \quad \text{(R5)}$$

While the reaction of N_2O_5 with water vapor is very slow, a considerable loss of N_2O_5 is assumed to occur on the surface of aqueous aerosol particles [*Platt et al.*, 1984].

$$N_2O_5 + H_2O \xrightarrow{aerosol} 2 \cdot HNO_3 \quad \text{(R6)}$$

The heterogeneous hydrolysis of N_2O_5 on the surface of aqueous aerosol particles thus represents another removal path for NO_x. It leads to HNO_3 formation like R1, and it competes with R4. Reaction R6 is usually implemented into chemical transport models as a first order loss:

$$\left.\frac{\partial[N_2O_5]}{\partial t}\right|_{het.} = -k_{N_2O_5} \cdot [N_2O_5]. \quad (1)$$

[10] The surface area dependent rate constant $k_{N_2O_5}$, which is necessary for a quantitative treatment of R6, is usually parameterized in the following way:

$$k_{N_2O_5} = \frac{1}{4} \cdot c_{N_2O_5} \cdot S \cdot \gamma_{N_2O_5}, \quad \text{(P1)}$$

where $c_{N_2O_5}$ is the mean molecular velocity of N_2O_5, and S is the aerosol surface area density. For our calculations a

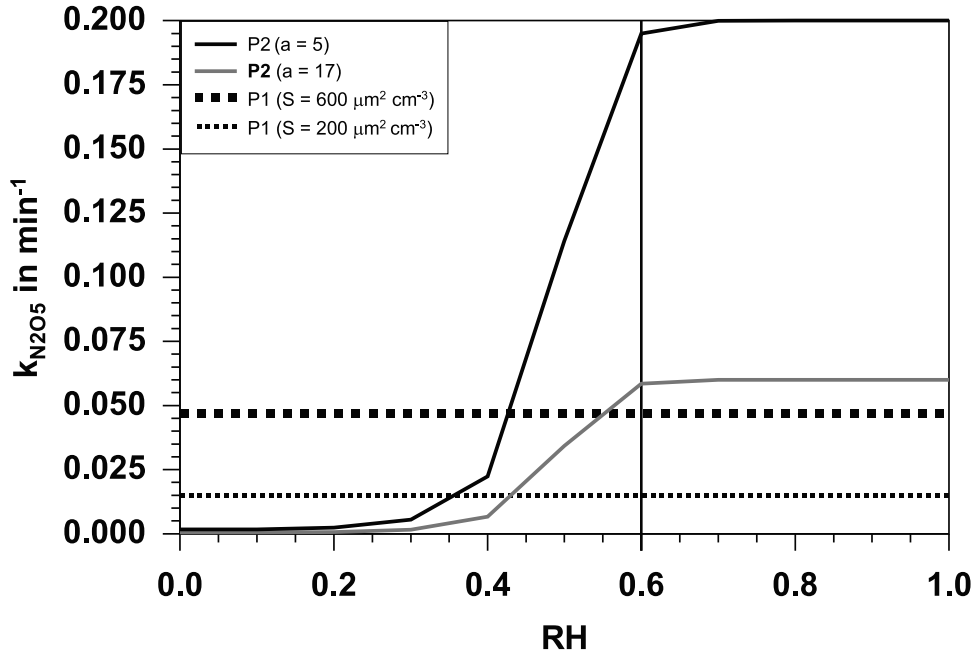

Figure 1. Rate constants for the heterogeneous hydrolysis of N_2O_5 when different parameterizations are used. See text for details.

diffusion correction according to the theory of *Fuchs and Sutugin* [1971] proved to be negligible. For γ_{N2O5} typical values are of the order of 10^{-2} [e.g., *Mozurkewich and Calvert*, 1988; *Hu and Abbatt*, 1997]. *Mentel et al.* [1999] show that γ_{N2O5} is on the order of one magnitude lower if the aerosol contains nitrate compared to sulfate aerosols. To include this effect we use in the following a basic value $\gamma_{N2O5} = 0.02$ as it was measured by *Mentel et al.* [1999], and to parameterize the nitrate effect we introduce a weighting of the reaction probability γ_{N2O5} according to the chemical composition of the aerosol:

$$\gamma_{N_2O_5,w} = f \cdot \gamma_1 + (1 - f) \cdot \gamma_2, \tag{2}$$

with $\gamma_1 = 0.02$, $\gamma_2 = 0.002$, and

$$f = \frac{m_{SO_4^{2-}}}{m_{SO_4^{2-}} + m_{NO_3^-}}. \tag{3}$$

[11] $m_{SO_4^{2-}}$ and $m_{NO_3^-}$ are the aerosol mass concentrations of sulfate and nitrate. If parameterization P1 is used with the weighted reaction probability $\gamma_{N2O5,w}$P1 will be referred to as P1*. We present results of both parameterizations, that is, with and without the nitrate effect.

[12] In the past several chemical transport models did not include an explicit treatment of the atmospheric aerosol. Therefore an alternative parameterization of $k_{N_2O_5}$ was commonly used. For example, *Chang et al.* [1987] proposed the following:

$$k_{N_2O_5} = \frac{1}{600 \ \exp\left(-\left(\frac{RH}{28}\right)^{2.8}\right) + a}. \tag{P2}$$

[13] RH is the relative humidity in % and $k_{N_2O_5}$ results in min^{-1}. *Chang et al.* [1987] used $a = 5$, which gives an asymptotic $k_{N_2O_5}$ of 0.2 min^{-1} if the relative humidity exceeds 60%. Figure 1 shows $k_{N_2O_5}$ as a function of the relative humidity. The parameterization P2 is based on the assumption that the relative humidity is an indicator for the aerosol surface area density and that $\gamma_{N2O5} = 0.1$. In addition, the values of $k_{N_2O_5}$ as they follow from P1 for different aerosol surface area densities ($S = 200$ μm^2 cm^{-3} and $S = 600$ μm^2 cm^{-3}) are given in Figure 1. Although the aerosol surface area density is far from being constant in the real atmosphere, we included the curves based on P1 for comparison. P1 will be identical to P2 at high relative humidity (RH > 60%), if the surface area density is about 2700 μm^2 cm^{-3}. However, such surface area densities can only be expected in highly polluted areas or if cloud droplets are present. Therefore P2 overestimates $k_{N_2O_5}$ under cloud free and unpolluted conditions. If we use $a = 17$ instead of $a = 5$ in P2, it is a much better approximation for P1, as can be seen from Figure 1. This point will also be addressed in section 4.2.

3. Box Model Simulations

[14] To investigate the importance of N_2O_5 hydrolysis with respect to photochemistry, box model runs were carried out for a simulation period of four days using RADM2 gas phase chemistry. The initial conditions, the diurnal cycles of the photolysis rates and the emissions of the reference simulation were identical to the PLUME1 case of the gas phase model intercomparison [*Kuhn et al.*, 1998]. The PLUME1 case was designed to test the chemistry in the moderately polluted air of the planetary boundary layer. It includes emissions for a variety of trace gases which are representative for continental European air [*Derwent and Jenkin*, 1991]. Temperature, relative humidity and pressure were kept constant during the simulations. Deposition and transport processes were not considered. We varied the NO emissions of the PLUME1 case by factors from 0.01 to 10 to investigate different ratios of volatile organic compounds and nitrogen oxides as well as different pollution levels.

[15] For the box model runs we prescribed the available surface area density, which remained constant during all the simulations. Figure 2 shows the maximum ozone values which were reached at the second day of the simulations together with the corresponding NO_y concentrations that were attained at the same time (here NO_y is the sum of the nitrogen containing species of RADM2; $NO_y = NO_x + HNO_3 + NO_3 + PAN + TPAN + HONO + HNO_4 + ONIT$. N_2O and particulate nitrate is not included.). The results of the simulations, where heterogeneous loss of N_2O_5 is not considered, are compared to those achieved with different parameterizations of the heterogeneous hydrolysis.

[16] In all cases it is obvious that the ozone concentration increases with increasing source strength up to a certain value of NO_y and then decreases again. In the following, the chemical conditions below and above this transition value are called the low-NO_x and high-NO_x regime, respectively. *Vogel et al.* [1999] have shown that the transition value of NO_y depends on various parameters, amongst them are meteorological parameters such as temperature and humidity as well as the ratio of VOC and NO_x. The low-NO_x regime does therefore not necessarily represent unpolluted conditions. For the simulations with parameterization P2, the relative humidity was always above 60%, which means that the hydrolysis was constantly present. As can be seen in Figure 2 also the treatment of the N_2O_5 hydrolysis affects the transition value. The arrows which indicate the low-NO_x and the high-NO_x regime in this picture refer to the standard simulation. The results show that the sensitivity of ozone toward the hydrolysis of N_2O_5 depends on the photochemical regime. Due to the N_2O_5 hydrolysis, NO_x is removed from the system, causing a decrease of ozone in the low-NO_x regime and an increase of ozone in the high-NO_x regime. This corresponds to the nonlinear behavior of the NO_x-HO_x-O_3 system. Figure 2 also illustrates that the parameterization P2 ($a = 5$) produces the largest differences, which can only be reached with the parameterization P1 if very large surfaces are available. On the whole, the highest sensitivity can be found in the high-NO_x regime. Here, the parameterization P1, which depends on the surface area density and the updated reaction probability, leads to differences in ozone concentration of up to 70% compared to the results where heterogeneous loss of N_2O_5 is not considered at all. The heterogeneous hydrolysis has an impact on the NO_x budget. In a previous study *Vogel et al.* [1999] discussed in more detail why in such a case the relative changes in the ozone concentrations are highest in the high-NO_x regime.

[17] For the pure chemistry runs and with respect to ozone we can conclude: (1) In the low-NO_x regime the heterogeneous hydrolysis of N_2O_5 leads to a decrease of ozone, but the relative change is small; (2) In the high-NO_x regime the heterogeneous hydrolysis of N_2O_5 leads to an increase of ozone and the relative change is quite large; (3) The commonly used parameterization based on older data of γ_{N2O5} is overestimating the effect of the heterogeneous hydrolysis of N_2O_5.

4. 1-D Simulations

[18] In the following, additional atmospheric processes such as turbulent transport and deposition are included. In order to obtain more realistic conditions, temporal changes of the emissions and of the atmospheric variables are allowed. This also means that the aerosol surface area density and the composition of the aerosol are both space and time dependent.

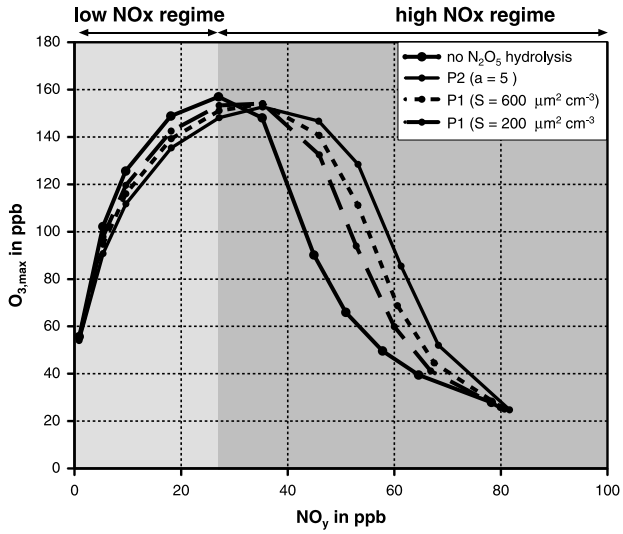

Figure 2. Ozone versus NO_y concentration when different parameterizations of the heterogeneous hydrolysis of N_2O_5 are applied. Results are also shown when heterogeneous hydrolysis of N_2O_5 is totally neglected.

[19] In all cases we use the aerosol model MADE, which is based on the Regional Particulate Model (RPM; *Binkowski and Shankar* [1995]) and provides detailed information about the chemical composition and the size of atmospheric particles as well as the dynamic processes influencing the particle population. The aerosol population of the submicron particles is represented by two overlapping modes, the Aitken mode and the accumulation mode, which are approximated by lognormal functions. In the model version used for the KAMM/DRAIS simulations, only secondary inorganic aerosol is considered (neither primary inorganic aerosol nor organic aerosol), and we implemented the N_2O_5 reaction according to the parameterizations P1 and P1* into the aerosol module MADE. The chemical composition of the aerosol phase consists of an internal mixture of SO_4^{2-}, NH_4^+, NO_3^- and water. The binary nucleation of sulfuric acid and water is implemented as a source mechanism. Coagulation, condensation, turbulent diffusion and deposition modify the aerosol population spatially and temporary. The aerosol surface area density, and therefore $k_{N_2O_5}$, is time and height dependent. We do not consider mineral dust and sea salt aerosol. Mineral dust will be included in the EURAD/MADE simulations for the European scale. It shows that these coarse mode species contribute only very little to the active surface area. For the KAMM/DRAIS model domain this contribution is expected to be even smaller. Moreover, the reaction probability for N_2O_5 on NaCl is very small as well as it is shown by *Behnke et al.* [1997].

[20] To investigate the effect of vertical diffusion only, a fully coupled 1-D version of the comprehensive mesoscale model system KAMM/DRAIS is applied. In the vertical direction 45 layers are used. The vertical grid size varies from 17 m close to the surface up to 400 m at the top of the

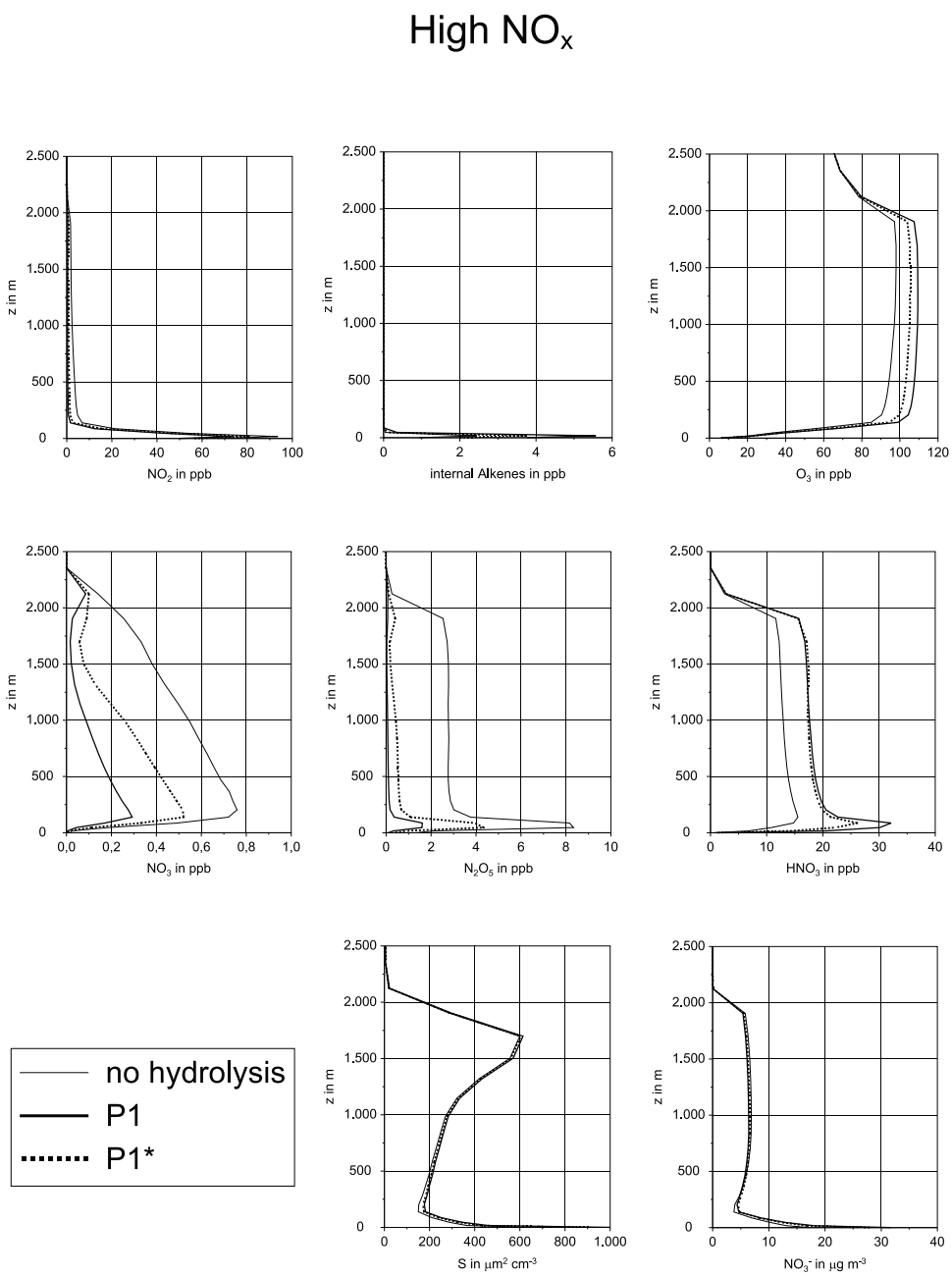

Figure 3a. Simulated vertical profiles of NO_2, internal alkenes, O_3, NO_3, N_2O_5, HNO_3, aerosol surface area density S, and NO_3^- for individual parameterizations of the heterogeneous hydrolysis of N_2O_5 at 0300 CET.

model domain at 12 km above sea level. The time steps are on the order of seconds. The whole model system runs in a fully coupled mode. For this study we focused on a cloudless situation under typical summer conditions with relative humidity above 55%. The gas phase emissions are time dependent and represent the conditions of a moderately polluted area in Europe. We investigated two emission scenarios, a low-NO_x case and a high-NO_x case. In the high-NO_x case the NO_x emissions used for the low-NO_x case were multiplied by a factor of 7. This corresponds to a heavily polluted environment.

[21] Simulations were performed without the heterogeneous hydrolysis of N_2O_5 and with the hydrolysis reaction using parameterization P1 and P1*. The individual runs were carried out for several days to eliminate the influence of the initial conditions. We will concentrate on the results of day 3 when the peak ozone concentrations reach typical ozone episode values for Central Europe.

4.1. Simulated Profiles

[22] We first investigate the nighttime profiles of those species which are involved in N_2O_5 production or which are directly affected by the heterogeneous hydrolysis of N_2O_5. Figure 3a presents vertical concentration profiles of NO_2, the internal alkenes (model species OLI), O_3, NO_3, N_2O_5, HNO_3, the aerosol surface area density including water, and

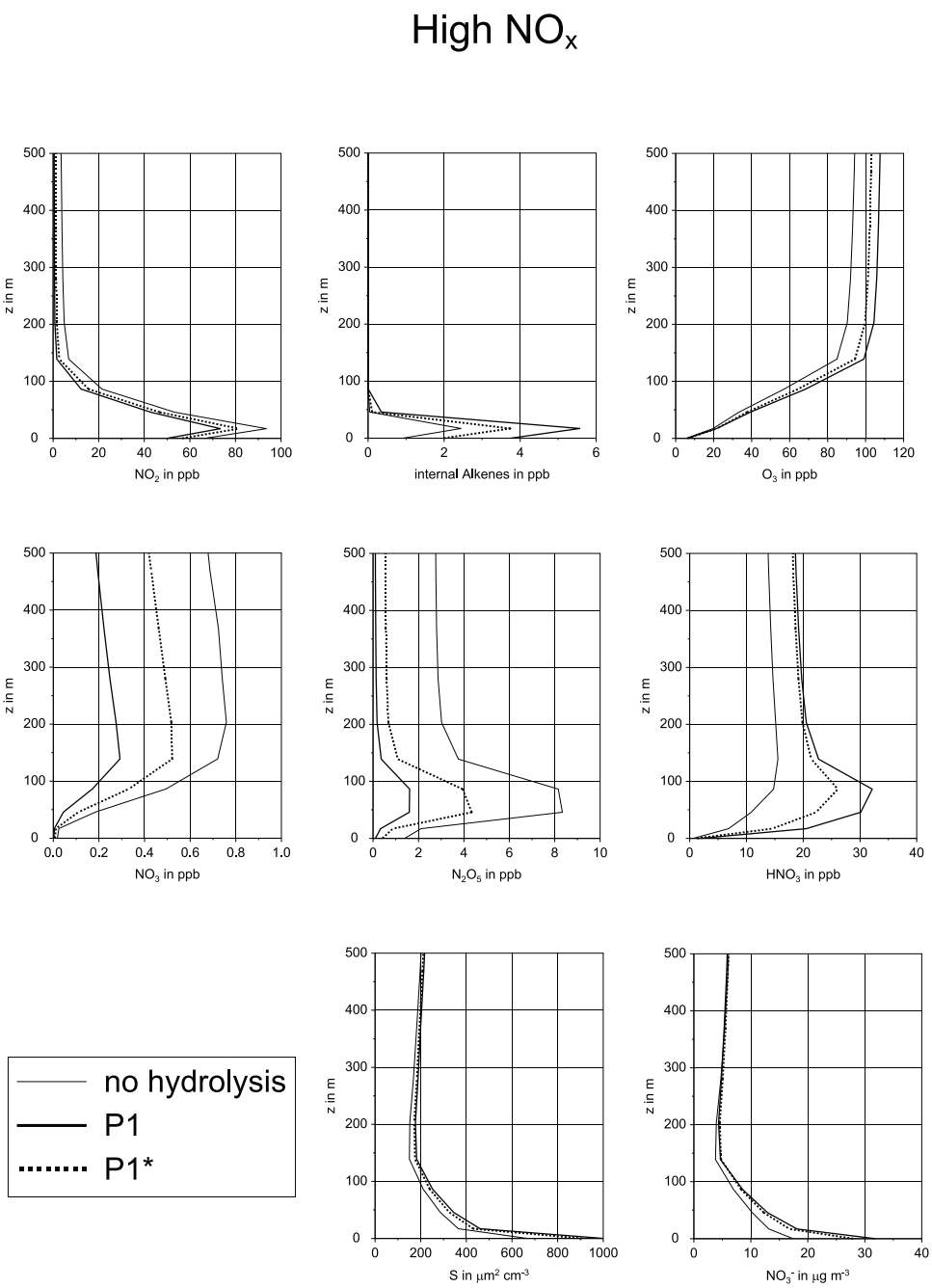

Figure 3b. Same as Figure 3a but for the height interval 0–500 m.

the nitrate content of the aerosol particles at 0300 CET for the high-NO_x case and for the individual treatments of the heterogeneous hydrolysis of N_2O_5. At this time the nocturnal boundary layer has a height of 139 m and the residual layer above reaches 2000 m. NO_2, O_3, and NO_3 are presented as precursors of N_2O_5. HNO_3 is shown as a product of the heterogeneous hydrolysis of N_2O_5. In addition its gas phase concentration has an influence on the nitrate content of the aerosol. The internal alkenes are chosen as a representative of VOC because the emissions of terpenes, which are occurring during the whole night, are lumped into this RADM2 class. The internal alkenes also react with NO_3 directly. The aerosol surface area density determines the rate of hydrolysis of N_2O_5 and is therefore also shown in Figure 3a.

[23] The aerosol surface area density reaches its maximum values in the upper part of the residual layer and close to the surface during nighttime. There are two primary reasons for this. First, the formation of ammonium nitrate, which depends on the availability of NH_3 and HNO_3, on temperature, and on the relative humidity (low temperature and high relative humidity favor the formation of ammonium nitrate). Second, the uptake of water vapor that increases the aerosol surface area density is enhanced by high relative humidity, which occurs in these layers.

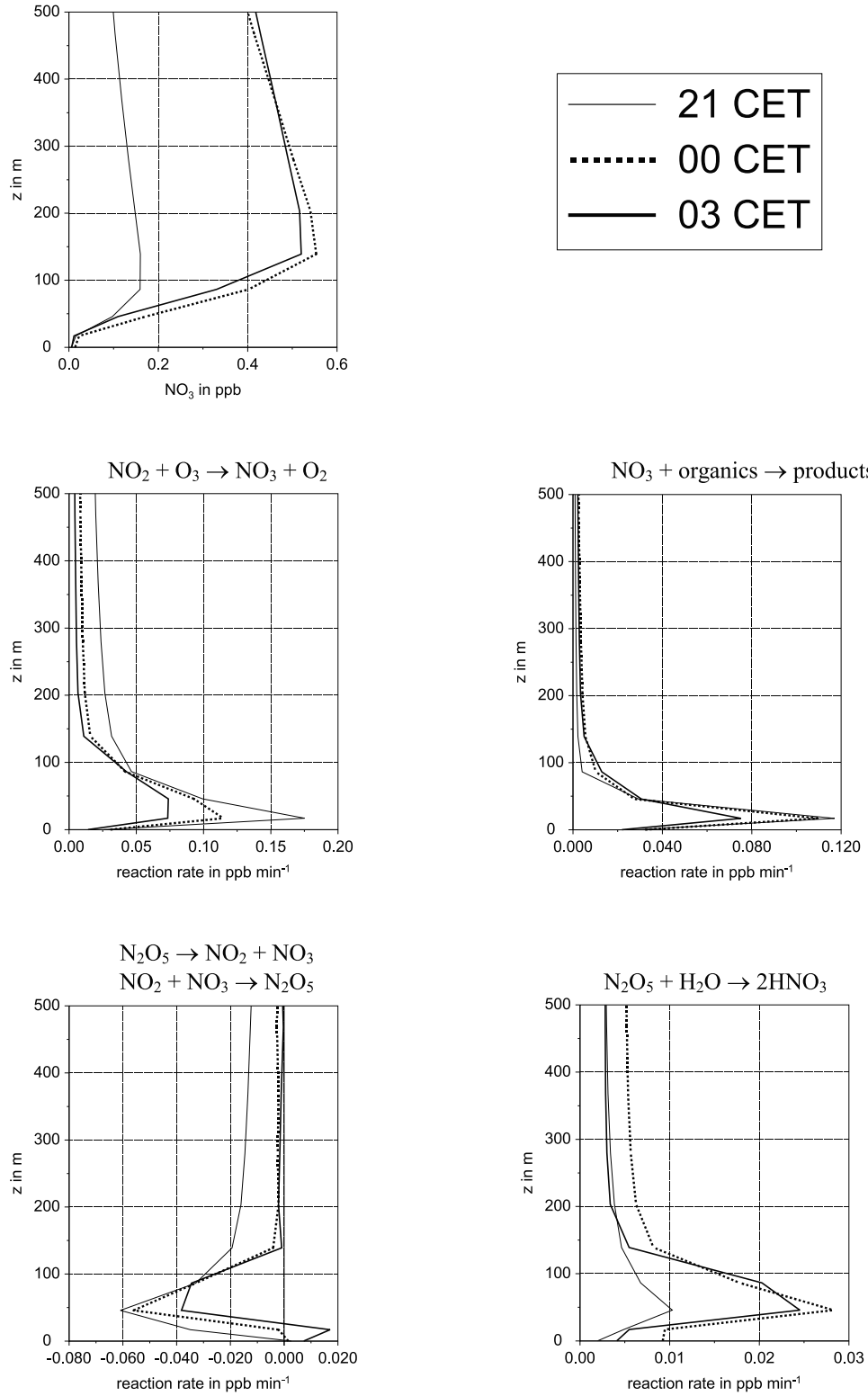

Figure 3c. Same as Figure 3b but for NO_3 and for the reaction rates of individual reactions at 2100, 0000, and 0300 CET (P1*).

[24] Figure 3b shows the same situation but up to a height of 500 m for a better resolution of the nocturnal boundary layer. We first concentrate on the results where the parameterization P1* was applied to treat the heterogeneous hydrolysis of N_2O_5. Since NO_x and the internal alkenes are mainly emitted close to the surface, NO_2 and the internal alkenes have their maximum concentration close to the surface. Both are decreasing with height, but the decrease of the internal alkenes occurs more rapidly than that of NO_2 because of additional reaction of the

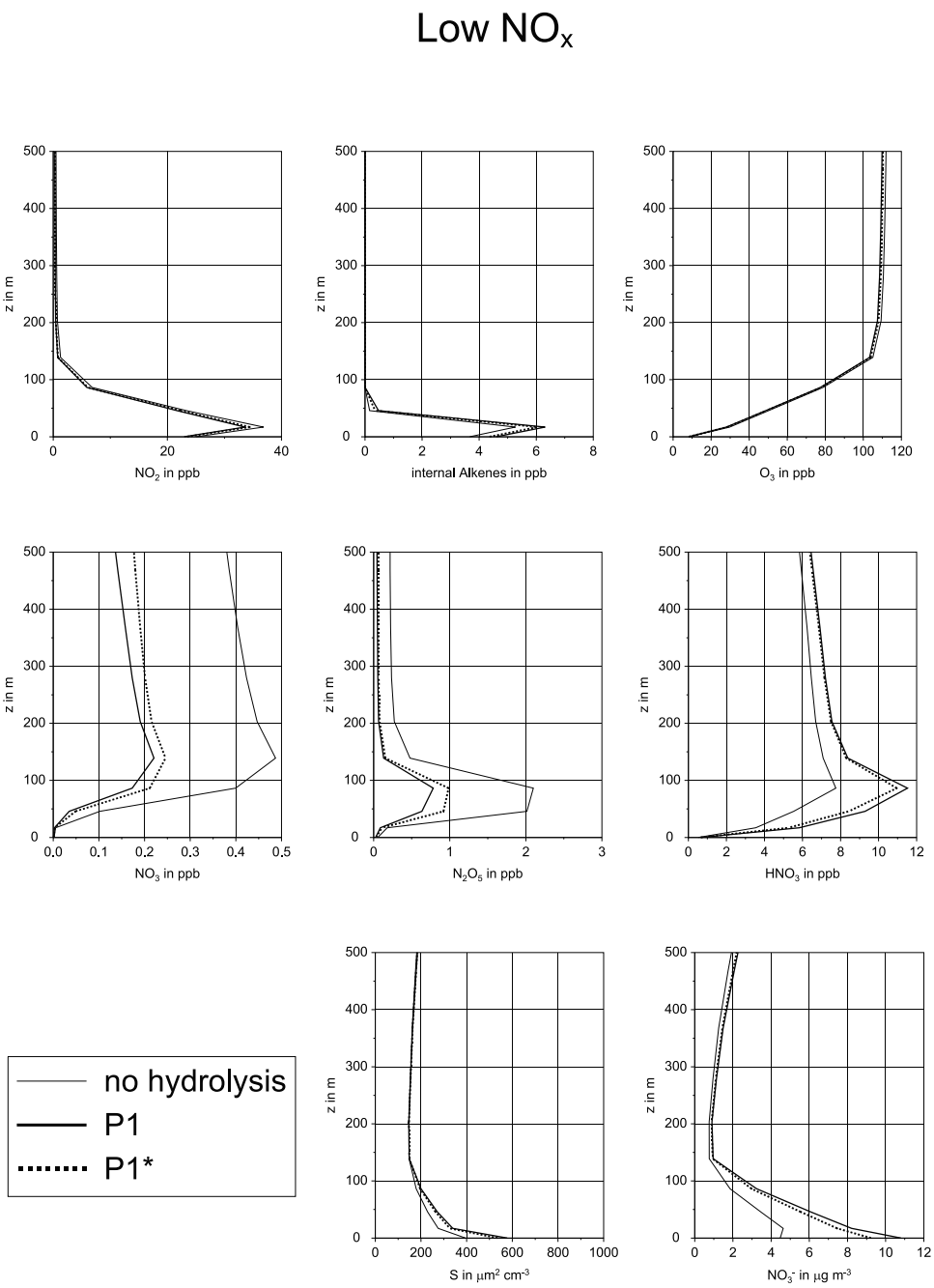

Figure 3d. Same as Figure 3b but for the low-NO_x case.

alkenes with O_3 and the ongoing conversion of NO to NO_2 in these heights.

[25] During the night ozone is depleted within the nocturnal boundary layer, which reaches a height of 139 m. The reduced vertical mixing, the reaction of ozone with freshly emitted NO and the deposition of ozone at the surface all lead to a steep vertical gradient. Within the residual layer the high ozone concentrations of the day before still exist.

[26] NO_3 has a maximum at 139 m above the surface, which is at the top of the nocturnal boundary layer in the investigated case. N_2O_5 is formed during nighttime, reaching its maximum concentration at a height of approximately 50 m above the surface. Above 90 m N_2O_5 decreases very rapidly and is almost constant above 200 m in the residual layer. In contrast to N_2O_5, NO_3 only decreases slowly with height. HNO_3 shows a maximum at 90 m above the surface.

[27] In order to obtain a better insight into the ongoing processes during the night, Figure 3c gives vertical profiles of the NO_3 concentration and the rates of individual reactions, which are involved in the N_2O_5-NO_3 chemistry at different points of time (2100, 0000, and 0300 CET). Again we consider the profiles determined with the parameterization P1*.

[28] Above the nocturnal boundary layer, NO_3 starts to build up after sunset. At midnight, when the NO_3 concentration reaches its maximum, the nocturnal boundary layer reaches a height of 139 m. NO_3, which is found above the nocturnal boundary layer in the morning hours, has already

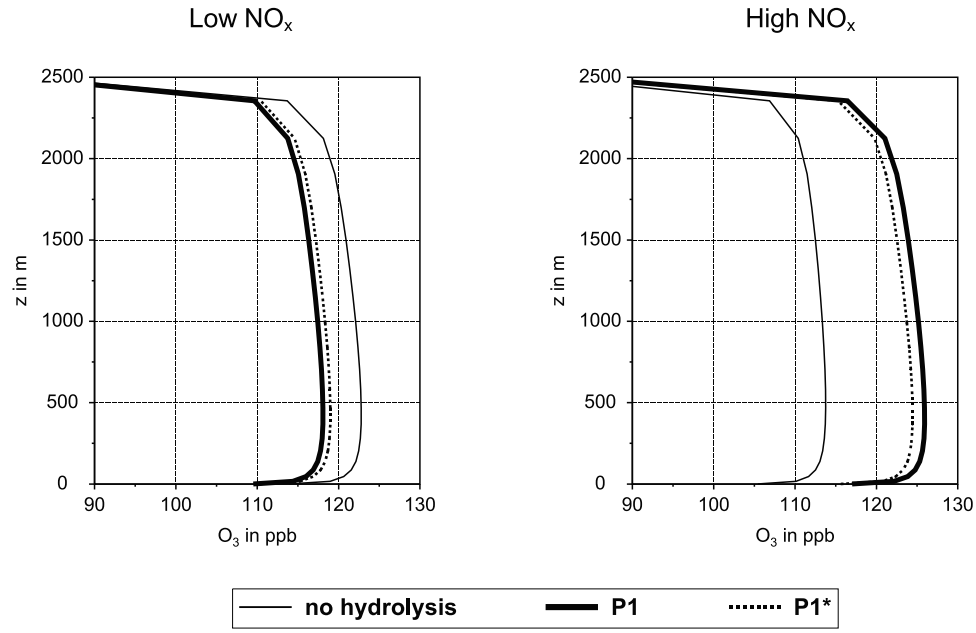

Figure 4. Simulated vertical profiles of O_3 at 1400 CET for individual parameterizations of the heterogeneous hydrolysis of N_2O_5.

been produced before midnight. When the NO_2 in the residual layer is almost consumed by the reaction with ozone, the production of NO_3 ceases. Since the concentration of O_3 is constant with height in the residual layer, the profiles of the production of NO_3 reflect the profiles of NO_2 above the nocturnal boundary layer.

[29] To explain the NO_3 profile within the nocturnal boundary layer we must quantify the contributions of the individual reactions. For this purpose Figure 3c shows the vertical profiles of the rates of the reaction of NO_2 with ozone (R2), the rate of the reaction of NO_3 with VOCs (R5), and the change of NO_3 due to reactions R3 and R4. A loss of NO_3 by reactions R3 and R4 (negative values in Figure 3c) indicates an identical chemical production of N_2O_5.

[30] Although the NO_3 production via reaction R2 is very effective within the nocturnal boundary layer, the competing reaction of NO_3 with VOC (R5) leads to low net production rates of NO_3 at this height interval. We looked at the daily cycles of the reaction rates of the individual VOC components with NO_3. From that analysis we found, that close to the surface and during night the reaction of internal alkenes with NO_3 is the main sink. During night the internal alkenes mainly consists of terpenes since the anthropogenic emissions are small compared to the biogenic ones. With increasing height the reaction with aldehydes becomes more important. However, the reaction rates are an order of magnitude smaller.

[31] Later at night, close to the surface, the production of NO_3 is slowed down further because ozone has been used up by the reaction with NO and therefore cannot act as a reaction partner for NO_2 anymore. The interaction of the production and the loss processes causes the NO_3 maximum to be located at 139 m at 0300 CET. It is clear that the profiles of NO_3 and the other species shown in Figures 3a and 3b do not reflect the chemical reactions only, but also the process of vertical diffusion, which is small during the night, but still present. The distinct maximum of NO_3 at the top of the nocturnal boundary layer is in good agreement with observations carried out in Heidelberg by *Friedeburg et al.* [2001].

[32] The profile of N_2O_5 is determined by the net effect of the rates of reactions R3 and R4 and by the heterogeneous hydrolysis of N_2O_5 (R6). Both are shown in Figure 3c, which displays a sharp maximum of production of N_2O_5 at 50 m above the surface. This height is determined by the coinciding availability of NO_2 and NO_3.

[33] The vertical profiles show that both, NO_3 and HNO_3, decrease more slowly with height than N_2O_5 does (Figure 3b). In the residual layer HNO_3 is still remaining from the day before. During the night, HNO_3 also constantly builds up because it is produced by the reaction of NO_3 with organics and by the reaction of NO_3 and HO_2.

[34] Comparing the results of the high-NO_x case (Figure 3b) with the results of the low-NO_x case (Figure 3d), we find that in the high-NO_x case the concentrations of all components (with the exception of O_3) are significantly higher than in the low-NO_x case, since nitrogen oxides are more abundant. A change in the NO_x levels also has implications for the particle phase. The corresponding aerosol surface area densities reach higher values in the high-NO_x case (1000 μm^2 cm^{-3} in the high-NO_x case versus 600 μm^2 cm^{-3} in the low-NO_x case, both cases with hydrolysis.) because more nitrate and water are present in the particle phase.

[35] Comparing the afternoon profiles of ozone, which are simulated with and without the heterogeneous hydrolysis of N_2O_5, we find qualitatively similar results to those of the box-model runs. This means that ozone decreases in the low-NO_x case and it increases in the high-NO_x case if the heterogeneous hydrolysis of N_2O_5 is taken into account (Figure 4). The overall impact in the high-NO_x regime exceeds the one in the low-NO_x regime. However, the differences are generally smaller than for the box model simulations.

[36] Concerning the influence of the heterogeneous hydrolysis of N_2O_5, the results are the following. As expected, N_2O_5, NO_3, and NO_2 are reduced if the heterogeneous hydrolysis of N_2O_5 is taken into account, whereas HNO_3, the aerosol surface area density, and the nitrate content of the aerosol are increased. Comparing the individual profiles with and without the heterogeneous hydrolysis of N_2O_5, we found: (1) The aerosol surface area density and the nitrate content of the aerosol increase considerably in the nocturnal boundary layer if the heterogeneous hydrolysis of N_2O_5 is taken into account. This is valid for the high-NO_x and the low-NO_x cases; (2) Large differences in HNO_3 occur at all heights up to the top of the residual layer. When the nitrate effect is taken into account, large differences are only found in the high-NO_x regime and in the nocturnal boundary layer; (3) We found a large impact on N_2O_5 in the low-NO_x and the high-NO_x regime and from the surface to the top of the boundary layer; (4) The concentration of NO_3 is considerably influenced by the heterogeneous hydrolysis of N_2O_5 at all heights. This should have an enormous influence on nighttime chemistry. Our process studies have shown that NO_3 is most important close to the surface, although the NO_3 concentrations there are very small. The reason for this is that large amounts of NO_3 are produced close to the surface during the night but are consumed by VOCs at the same time; (5) Compared to the nitrogen compounds mentioned before, the impact of the heterogeneous hydrolysis on the ozone concentration is relatively small. By analyzing the vertical profiles of N_2O_5 and the aerosol surface area density, it is clear that the sensitivity to the N_2O_5 hydrolysis is smaller in the 1-D case than in the box model runs because N_2O_5 and aerosol surface area density do not coincide in space.

[37] Comparing the profiles that were calculated with parameterizations P1 and P1* we found: (1) For the low-NO_x regime the differences are small if the nitrate effect is neglected; (2) In the high-NO_x regime large differences are found for the species NO_3, N_2O_5 and HNO_3. Therefore, we recommend taking into account the nitrate effect in three-dimensional simulation models to avoid large errors, especially under heavily polluted conditions.

[38] Although the effect of the heterogeneous hydrolysis of N_2O_5 on ozone is small, it is important for atmospheric chemistry for several reasons. It modifies the gas phase concentration of HNO_3 and therefore the nitrate content of the aerosol particles. In addition, it has a tremendous effect on the concentration of NO_3, which is the most important radical of nighttime chemistry [*Geyer et al.*, 2000, 2001].

4.2. Usefulness of Parameterization P2

[39] We have shown in section 3 that the parameterization P2 with $a = 17$ instead of $a = 5$ might give similar results as parameterization P1 if the relative humidity and the aerosol surface area density are highly correlated. In order to check how far this is valid Figure 5 gives vertical profiles of $k_{N_2O_5}$ for parameterization P1* and different versions of parameterization P2 for the high-NO_x case. It shows that the agreement of parameterization P2 compared to parameterization P1* increases if $a = 17$ is used. However, there is still a difference by a factor of two. This means, that parameter a depends on the individual situation and an universal value for this parameter cannot be determined.

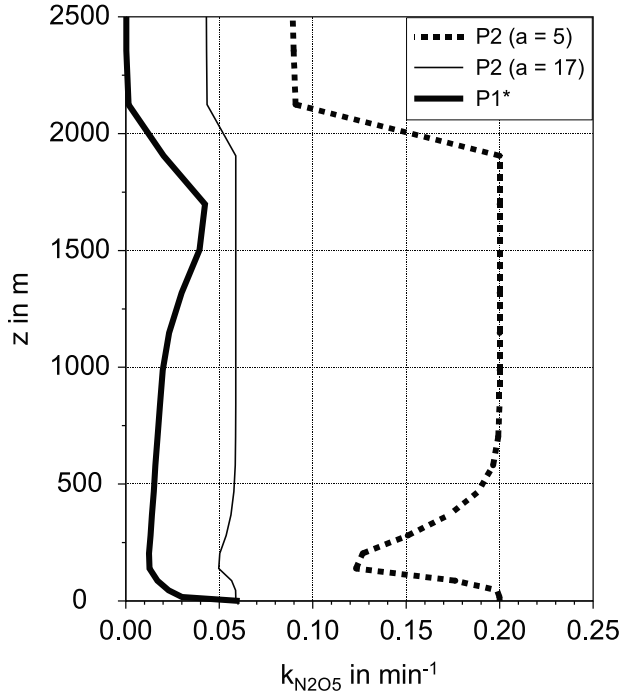

Figure 5. Vertical profiles of the rate constant of reaction R5 (equation (2)) for parameterizations P1* and P2 with $a = 5$ and $a = 17$, respectively.

5. 3-D Simulations

[40] As a next step we carried out three-dimensional simulations to study the role of the heterogeneous hydrolysis of N_2O_5 including now all processes treated by the model. First, a mesoscale model is used to investigate a typical summer smog situation neglecting cloud processes. For these simulations the KAMM/DRAIS model was used. This model system typically covers areas of 200×200 km^2. Second, model simulations were performed on the European scale. These model simulations include cloud processes and were performed with the EURAD model. The simulations with the different grid resolutions and the different model domains were performed to have a large variety of atmospheric conditions and chemical mixtures. This is necessary to ensure that our conclusions about the importance of the heterogeneous hydrolysis are not limited to special situations but can be generalized.

5.1. The KAMM/DRAIS Model System

[41] The comprehensive KAMM/DRAIS model system uses the nonhydrostatic mesoscale model KAMM [*Adrian and Fiedler*, 1991] as the meteorological driver. It is coupled with a surface vegetation model developed by *Schädler* [1989]. This model part gives the lower boundary conditions for temperature and humidity. The submodule DRAIS calculates the transport and diffusion of the reactive trace species. For the treatment of the chemical reactions the RADM2 gas phase chemistry mechanism [*Stockwell et al.*, 1990] is incorporated. The photolysis rate coefficients are

determined with the radiation scheme of *Ruggaber et al.* [1994]. The anthropogenic emissions are precalculated and the biogenic VOC emissions are calculated depending on the land use, the modeled temperatures, and modeled radiative fluxes [*McKeen et al.*, 1991; *Lamb et al.*, 1987; *Vogel et al.*, 1995]. For the parameterization of the NO emissions from the soil a modified scheme of *Yienger and Levy II* [1995] is employed [*Ludwig et al.*, 2001]. Since the biogenic emissions strongly depend on light (isoprene) and especially on temperature, we take these variables directly from the meteorological part of the KAMM/DRAIS model system at every time step. Dry deposition is parameterized by means of a big-leaf multiple resistance model [*Baer and Nester*, 1993]. As for the one-dimensional simulations described in section 4, the aerosol model MADE [*Ackermann et al.*, 1998] is used to describe the aerosol dynamics and chemistry.

[42] The typical horizontal grid size for applications of KAMM/DRAIS is in the range of 1 to 5 km. In the vertical direction 25 layers are used. The vertical grid size varies from 20 m close to the surface up to 400 m at the top of the model domain, which is at 8 km above sea level. The time steps are on the order of seconds, and the whole model system runs in a coupled mode. This means that all model parts are running at the same time using the same numerical grid, the same numerical solvers, and the same physical parameterizations for the meteorological and transport model.

[43] The land use data are available with a horizontal resolution of 30×30 m^2. Consequently, the biogenic VOC and NO emissions and the deposition fluxes are calculated with that high resolution. The calculated emissions and deposition fluxes are then integrated over the grid size of the individual simulations using a technique described in *Vogel et al.* [1995]. Using this subgrid method, the high resolution of the land use data is utilized.

[44] As in all limited area models, boundary conditions play an important role. In this study the following procedure is used to determine the inflow boundary conditions for the chemical species. The emissions of the area sources inside the model domain are averaged along a strip 20 km wide along the inflow boundaries. An area source with a source strength of the averaged values is given at every grid point of the inflow boundary at every time step. At the inflow boundaries the complete 3-D equations are solved assuming that $\partial c_i/\partial x_j = 0$, where c_i is the concentration of species i and x_j is the coordinate perpendicular to the boundary. This means that all physical and chemical processes at the inflow boundaries are treated consistently with the rest of the model domain. Therefore, our inflow boundary conditions are based on the assumption that there is a homogeneous area upwind of the model domain with typical and identical emissions at each surface grid point. KAMM/DRAIS has been extensively validated against observations in the past [*Vogel et al.*, 1995; *Nester et al.*, 1995; *Fiedler et al.*, 2000; *Corsmeier et al.*, 2001].

5.1.1. Topography and Meteorological Conditions

[45] The model is applied to an area in southwestern Germany. It covers main parts of Baden-Württemberg and the adjacent regions. The terrain height differs from 110 m in the Rhine valley up to 1500 m in the southern part of the Black Forest and the Vosges mountains. The horizontal grid size used for these simulations is 4×4 km^2. The model domain covers an area of 248×248 km^2. A typical summer situation was simulated with a geostrophic wind of 4.5 m s^{-1} blowing from east. The solar radiation and the photolysis rate coefficients are calculated corresponding to 3 July. The maximum temperatures during the day are on the order of 30°C.

5.1.2. Emissions

[46] To carry out the simulations, data for the anthropogenic and biogenic emissions are necessary. The anthropogenic emissions of SO_2, CO, NO_x, NH_3 and 32 individual classes of VOC according to the RADM2 mechanism were precalculated with a spatial resolution of 1×1 km^2 and a temporal resolution of one hour. The anthropogenic emission data account for traffic emissions, emissions by large point sources and area sources such as households and industrial areas. The method used to determine these emissions is described by *Obermeier et al.* [1995], *Wickert et al.* [1999], *Pregger et al.* [1999], and *Seier et al.* [2000]. The biogenic emissions were calculated online as described above.

[47] Figure 6 shows the horizontal distributions of the emissions of SO_2, NO_x, VOC (anthropogenic and biogenic) and NH_3 at 0800 CET. While the emissions of SO_2 and NO_x reflect the locations of the urban areas and highways, the NH_3 emissions are concentrated in the rural areas of the model domain. Although the highest VOC emissions are found in the urban areas, they are much more homogeneously distributed than the emissions of the species mentioned before, due to the large contribution of biogenic VOC emissions in the domain.

5.1.3. KAMM/DRAIS Model Results

[48] Figure 7 shows the topography of the model domain and the wind field at 20 m above the surface at 1400 CET. The characteristics of the wind field are the channeling of the airflow in the Rhine valley and the thermal secondary flow systems on the slopes of the mountains. In the area of Freiburg the wind direction is 300° at that time, although the flow in the free troposphere is from the East. The maximum temperature in the Rhine valley reaches about 28°C. The relative humidity in the lowest model layer varies between 60% and 90% during the night and between 40% and 60% during daytime.

[49] To quantify the effect of the heterogeneous hydrolysis of N_2O_5 on chemistry and nitrate formation we carried out two model runs. The first model run describes the heterogeneous hydrolysis of N_2O_5 using parameterization P1*, that is, including the nitrate effect. The second model run does not take into account N_2O_5 hydrolysis at all.

[50] Similarly to section 4.1, we first look at the distributions of selected species at 0300 CET. Since only a limited number of figures can be presented here, we will show in the following the horizontal distributions of individual species at those heights where the maximum concentrations were found in section 4.1 (1-D studies). Figure 8a (top) shows the horizontal distribution of the concentration of N_2O_5 and the surface area density of the aerosol (bottom) at about 150 m above the surface for the reference case. It must be mentioned that the maximum surface area concentrations are found close to the surface. The N_2O_5 concentrations vary between almost zero ppb in the more remote areas and 1 ppb between Mannheim and Saarbrücken. The surface area density is in the range of

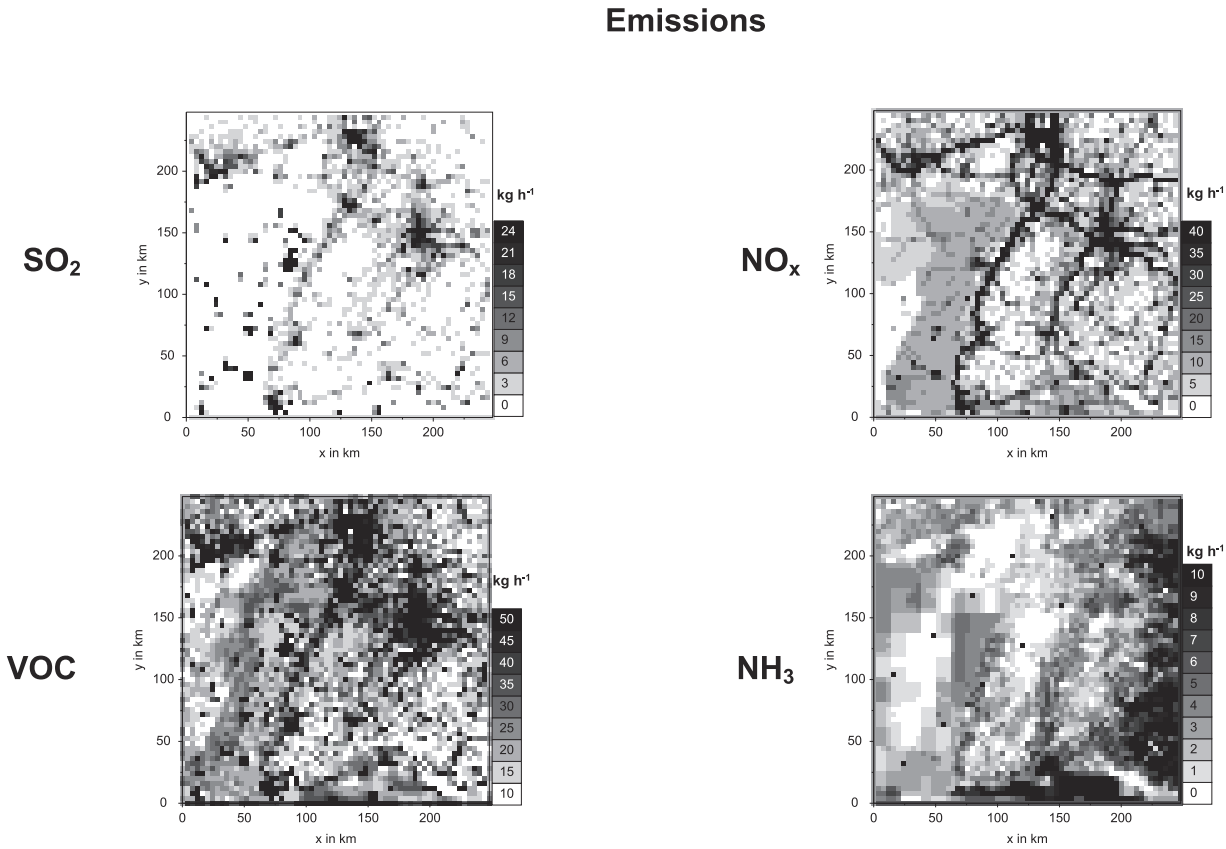

Figure 6. Horizontal distributions of the emissions of SO_2, NO_x, total VOC and NH_3 at 0800 CET. Numbers are given for areas of 4 × 4 km^2.

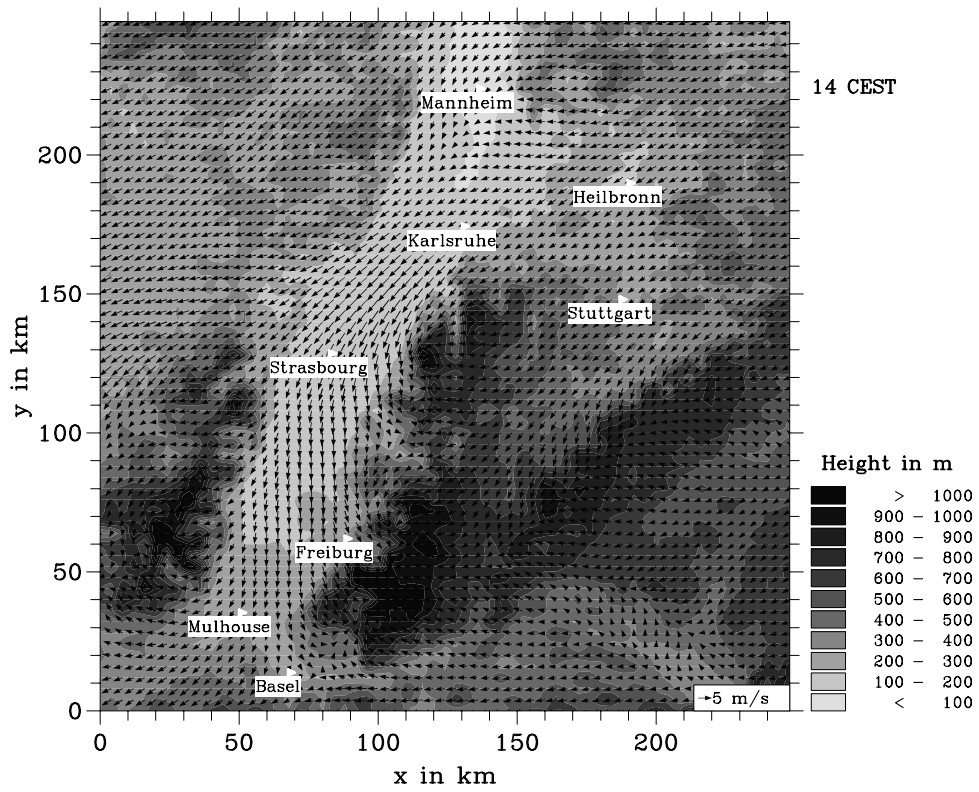

Figure 7. Topography of the model domain and wind field at 20 m above the surface at 1400 CET.

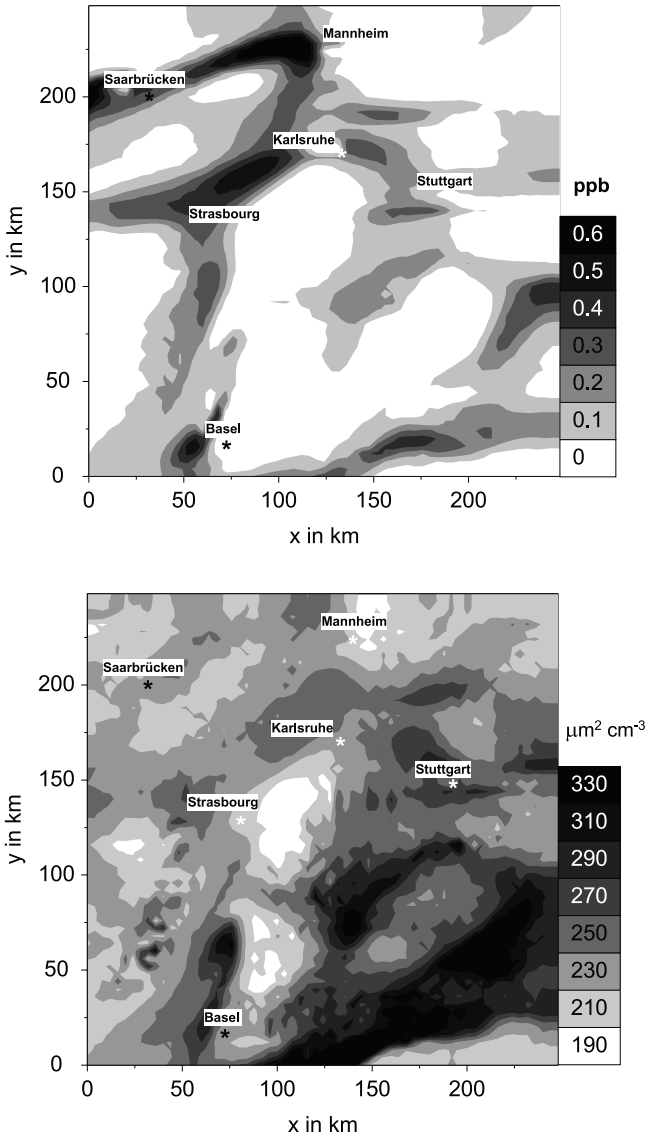

Figure 8a. Horizontal distribution of N_2O_5 (top) and the aerosol surface area density (bottom) at 150 m above the surface at 0300 CET.

185 μm^2 cm^{-3} and 510 μm^2 cm^{-3}. The highest values at this height are found in the southwestern part of the model domain where high amounts of ammonia are available. Figure 8a shows again that the shape of the horizontal distributions of N_2O_5 and the surface area density of the aerosol are different. Maximum values of N_2O_5 and the surface area density do not necessarily coincide. This diminishes the effect of the heterogeneous hydrolysis compared to the pure chemistry run presented in section 3.

[51] Figure 8b shows the horizontal distribution of NO_3 at about 350 m above the surface for the reference case at 0300 CET. At this height NO_3 varies between almost zero ppb in some parts of the Rhine valley and 0.12 ppb. In addition, Figure 8b (bottom) shows the reduction of NO_3 that occurs when the heterogeneous hydrolysis of N_2O_5 is taken into account. It is obvious that the largest reductions of NO_3 are found in those areas where NO_3 itself is high. On average we found a 70% reduction of NO_3 caused by the heterogeneous hydrolysis. Since the NO_3 chemistry is very important during the night [*Geyer et al.*, 2000, 2001], this underlines the importance of a correct treatment of the heterogeneous hydrolysis.

[52] Figure 8c shows the horizontal distributions of the nitrate content of the aerosol at 20 m above the surface for the case with N_2O_5 hydrolysis, together with the difference of the nitrate content of the aerosol when the heterogeneous hydrolysis is not considered. The nitrate content varies between zero μg m^{-3} in the western part of the model domain and 16 μg m^{-3} in the eastern part. If hydrolysis is taken into account the nitrate content of the aerosol increases remarkably compared to the case where hydrolysis is not considered (Figure 8c, bottom). In those areas where the nitrate content of the aerosol is low for the case without heterogeneous hydrolysis this increase reaches almost 200%. This shows again the necessity of a realistic treatment of the heterogeneous hydrolysis of N_2O_5.

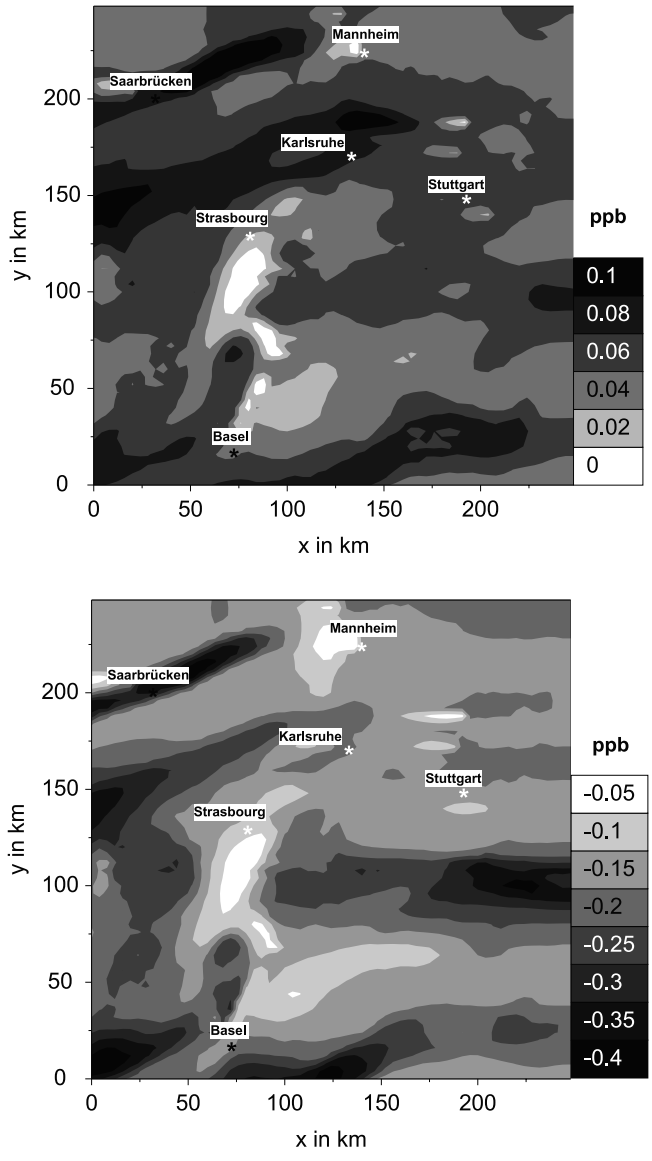

Figure 8b. Horizontal distribution of NO_3 (top) and ΔNO_3 (bottom) at 350 m above the surface at 0300 CET.

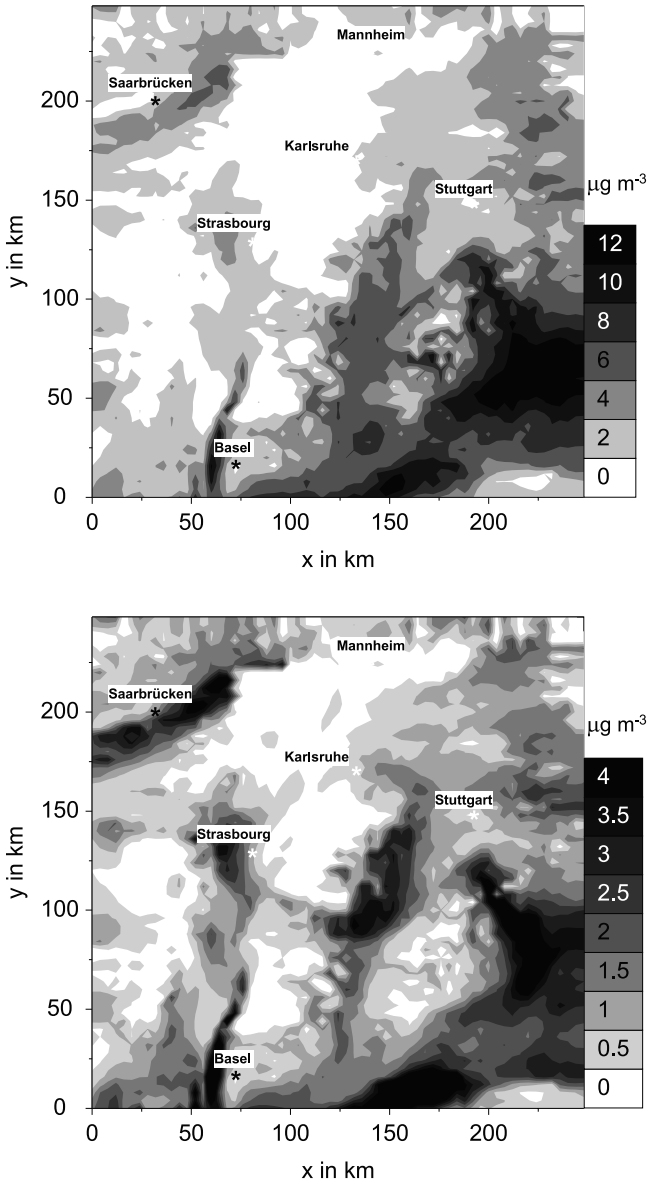

Figure 8c. Horizontal distribution of NO_3^- (top) and ΔNO_3^- (bottom) at 20 m above the surface at 0300 CET.

[53] Finally, we also investigated the effect of the hydrolysis on ozone during daytime. Figure 8d shows the horizontal distribution of the ozone concentration taking N_2O_5 hydrolysis into account and the difference in the ozone concentration if the heterogeneous hydrolysis is not considered (20 m above the surface at 1400 CET). The ozone concentration reaches maximum values of around 120 ppb. If the heterogeneous hydrolysis of N_2O_5 is taken into account, ozone concentrations are reduced in the entire model domain. In contrast to the box model and one-dimensional model studies no increase of ozone concentrations is found in the entire model domain although small fractions of the model domain are in the high-NO_x regime. The indicator H_2O_2/HNO_3 is applied to delimit the high NO_x-areas. The white contour line in Figure 8d indicates those areas where the ratio H_2O_2/HNO_3 reaches the value 0.2. According to *Hammer et al.* [2002] high-NOx conditions apply if this ratio falls below 0.2. In these areas an increase of O_3 would be expected, but transport of air masses from areas that belong to the low-NO_x regime leads to an overall decrease. This demonstrates the effect of horizontal transport on the ozone sensitivity with respect to the heterogeneous hydrolysis. The maximum decrease of the ozone concentration is on the order of 5%.

[54] From these results we conclude that the heterogeneous hydrolysis of N_2O_5 is more important for substances such as NO_3 and HNO_3 (which is not shown here) and the nitrate content of the aerosol than for the ozone concentration during summer smog episodes.

5.2. The EURAD/MADE Model System

[55] The comprehensive three-dimensional Eulerian EURAD/MADE model system is capable of predicting

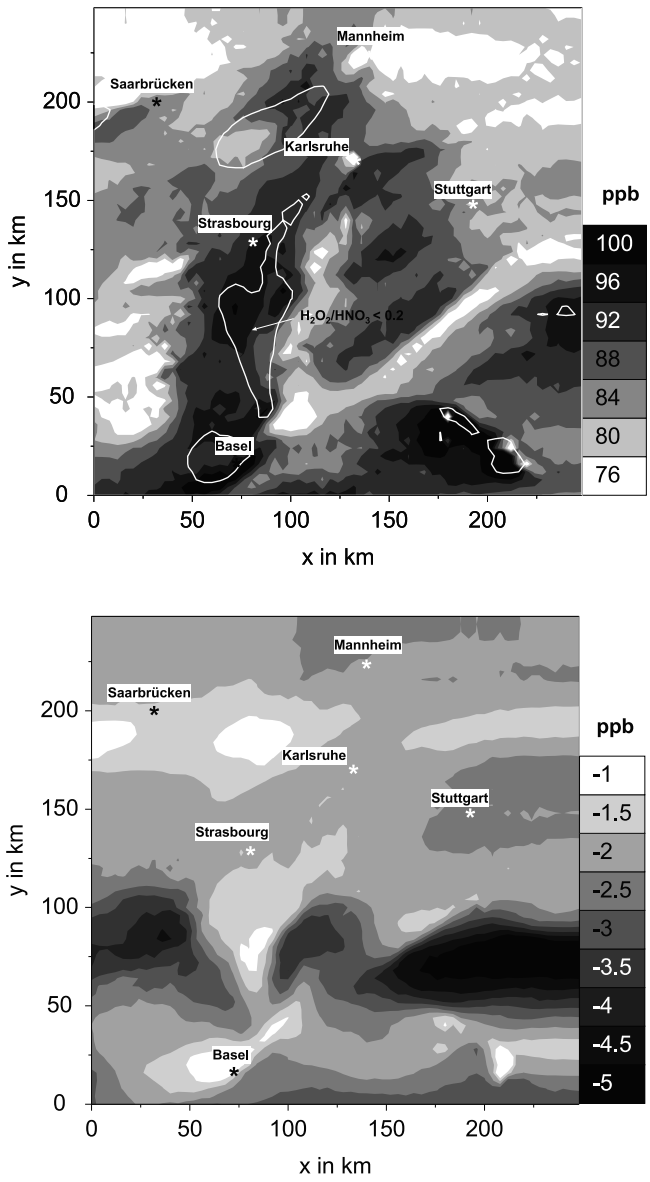

Figure 8d. Horizontal distribution of O_3 (top) and ΔO_3 (bottom) at 20 m above the surface at 1400 CET. The contour line in the O_3 distribution indicates where the ratio of H_2O_2/HNO_3 equals 0.2.

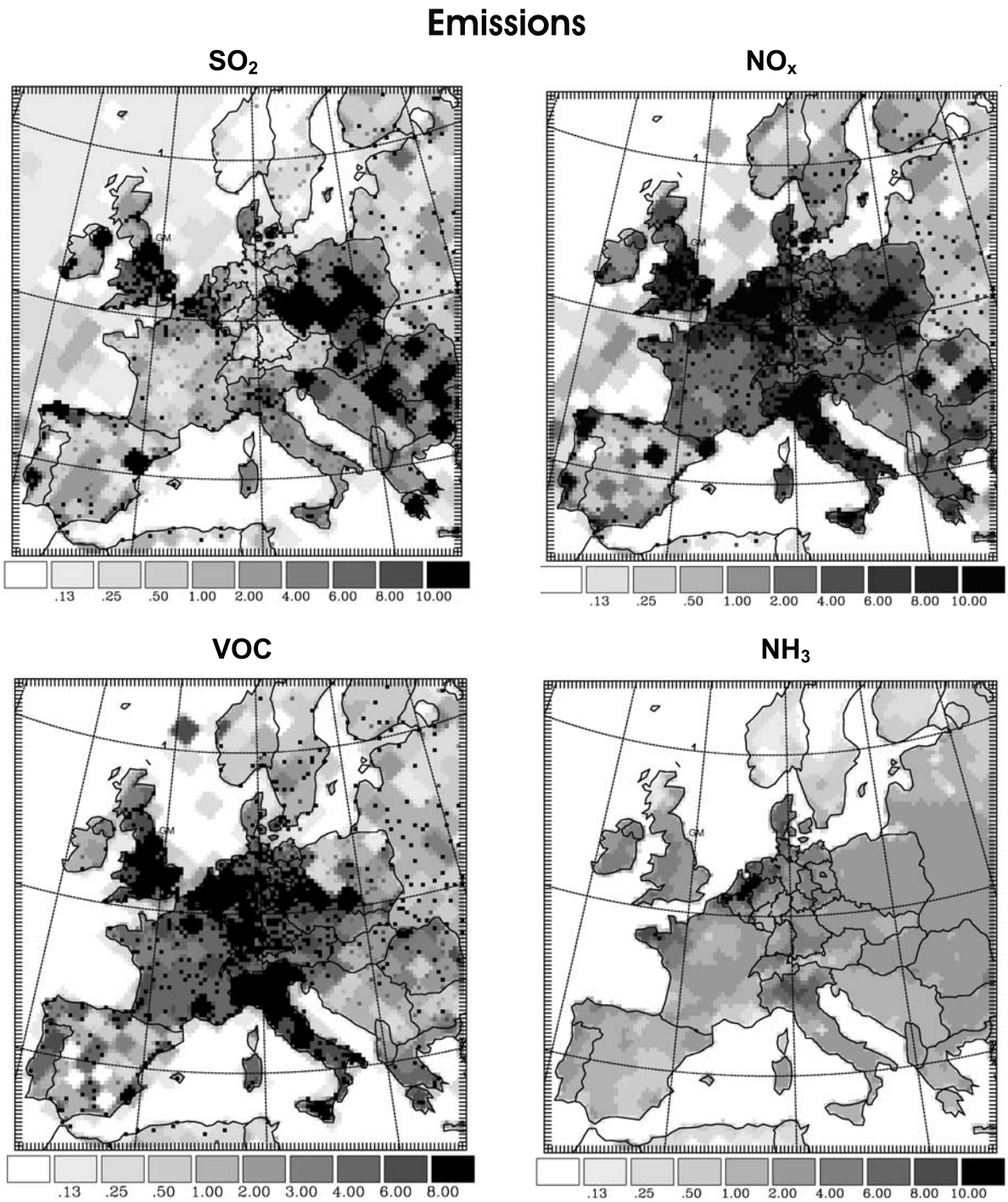

Figure 9. Horizontal distributions of SO_2, NO_x, anthropogenic VOC and NH_3 in tonnes per day for the EURAD/MADE simulations.

gas-phase concentrations of common trace gases and concentrations of particulate matter. EURAD consists of three major components: (1) the meteorological model MM5 [*Grell et al.*, 1994], (2) the EURAD emission model [*Memmesheimer et al.*, 1995], and (3) the chemistry-transport model CTM2 [*Hass et al.*, 1995; *Chang et al.*, 1987]. The EuroRADM gas-phase chemical mechanism [*Stockwell and Kley*, 1994], which is based on the RADM2 mechanism [*Stockwell et al.*, 1990], is used to take specific European features of the atmospheric chemistry into account. Furthermore, a more detailed description of the isoprene chemistry [*Zimmermann and Poppe*, 1996] and biogenic monoterpene chemistry [*Stockwell et al.*, 1997] are implemented into the gas-phase mechanism.

[56] As before, the aerosol dynamics model MADE is applied. The first model version was limited to submicron particles consisting of inorganic ions and water, but further model developments and the incorporation of the aerosol portion of MODELS-3 CMAQ [*Binkowski*, 1999] allow the treatment of the coarse particle size range and the cloud

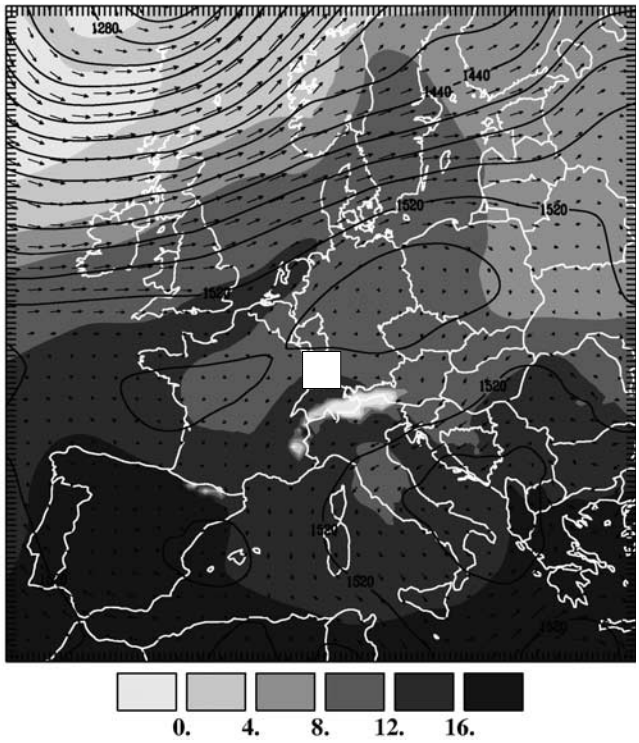

Figure 10. Geopotential height in m (isolines), temperature in °C (shading), and horizontal wind-vectors (maximum is 18.87 m s^{-1}) at 850 hPa at 0000 UTC (7 July 1995) as simulated with the MM5 for the EURAD/MADE model domain. The shaded rectangular indicates the location of the KAMM/DRAIS domain.

processing of aerosols. Aerosol-cloud interaction contains vertical redistribution of number and mass of all modes, impaction scavenging (number and mass of Aitkenmode and accumulation modes), sulfate production in the aqueous phase (only accumulation mode mass) and wet deposition (number and mass of accumulation and coarse mode). Additionally, a detailed description of anthropogenic and biogenic secondary organic aerosol formation has been implemented [*Schell et al.*, 2001].

5.2.1. Model Domain and Simulated Episode

[57] The EURAD/MADE model system is applied to simulate a long-term period covering essentially the growing season in the year 1995 (April to September). The coarse domain covers Europe with a horizontal grid resolution of 27 km. The vertical direction is resolved by 15 levels between the Earth's surface and 100 hPa using a $\sigma-$ coordinate system. The planetary boundary layer is represented by approximately 10 layers in the vertical and the thickness of the near surface layer is about 35 m. To investigate the influence of the N_2O_5 hydrolysis a 3-day episode in July has been chosen (5 July to 7 July 1995) using the parameterization P1*. The results of this simulation are compared to results of a simulation where N_2O_5 hydrolysis is not considered.

5.2.2. Emissions

[58] The EURAD emission model (EEM) is applied to calculate the temporal and spatial distribution of anthropogenic emissions of SO_2, NO_x, CO, NH_3, classes of VOC according to the RADM2 mechanism, and primary particles. The gas phase emission inventory is based on the national totals for 1995 provided by the Auto-Oil II program [*European Commission*, 2000] combined with the spatial information provided by EMEP [*EMEP*, 1998].

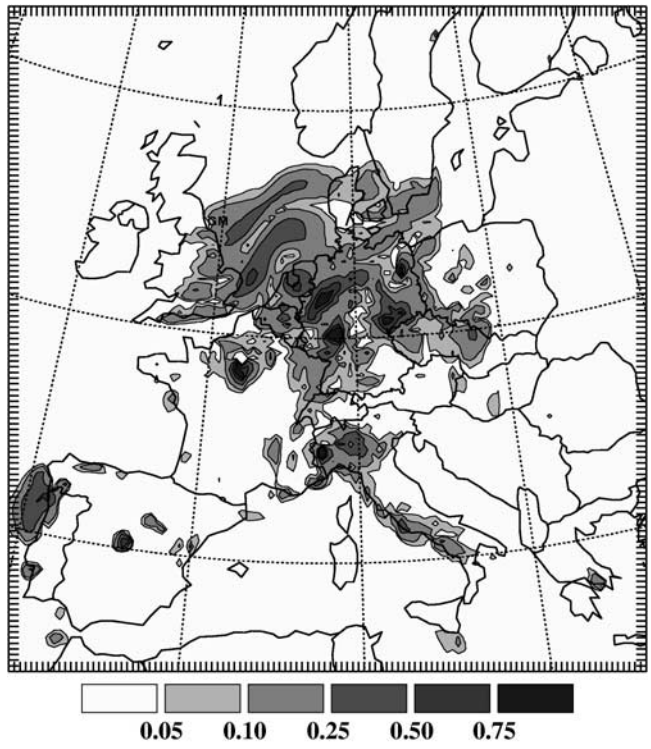

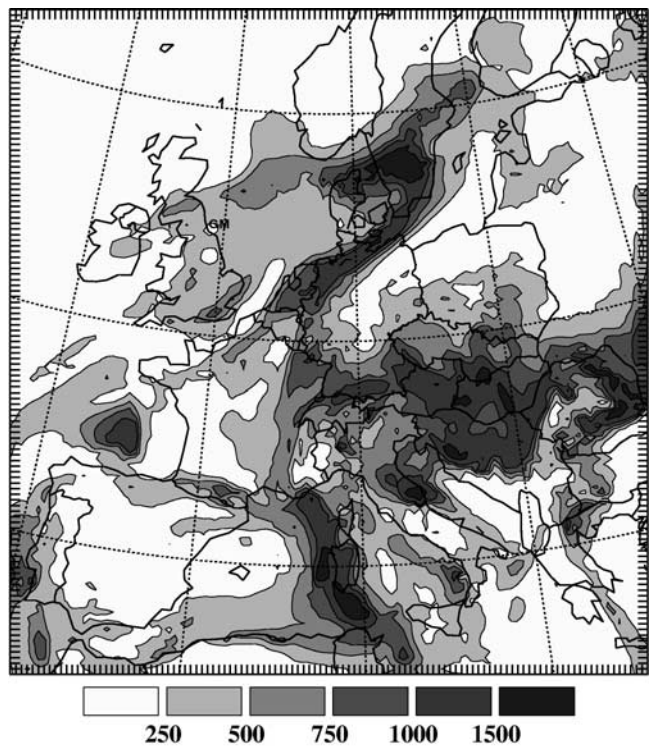

Figure 11a. Horizontal distribution of N_2O_5 (top) in ppb and the aerosol surface area density (bottom) in μm^2 cm^{-3} at 130 m above the surface at 0000 UTC for the EURAD/MADE simulation.

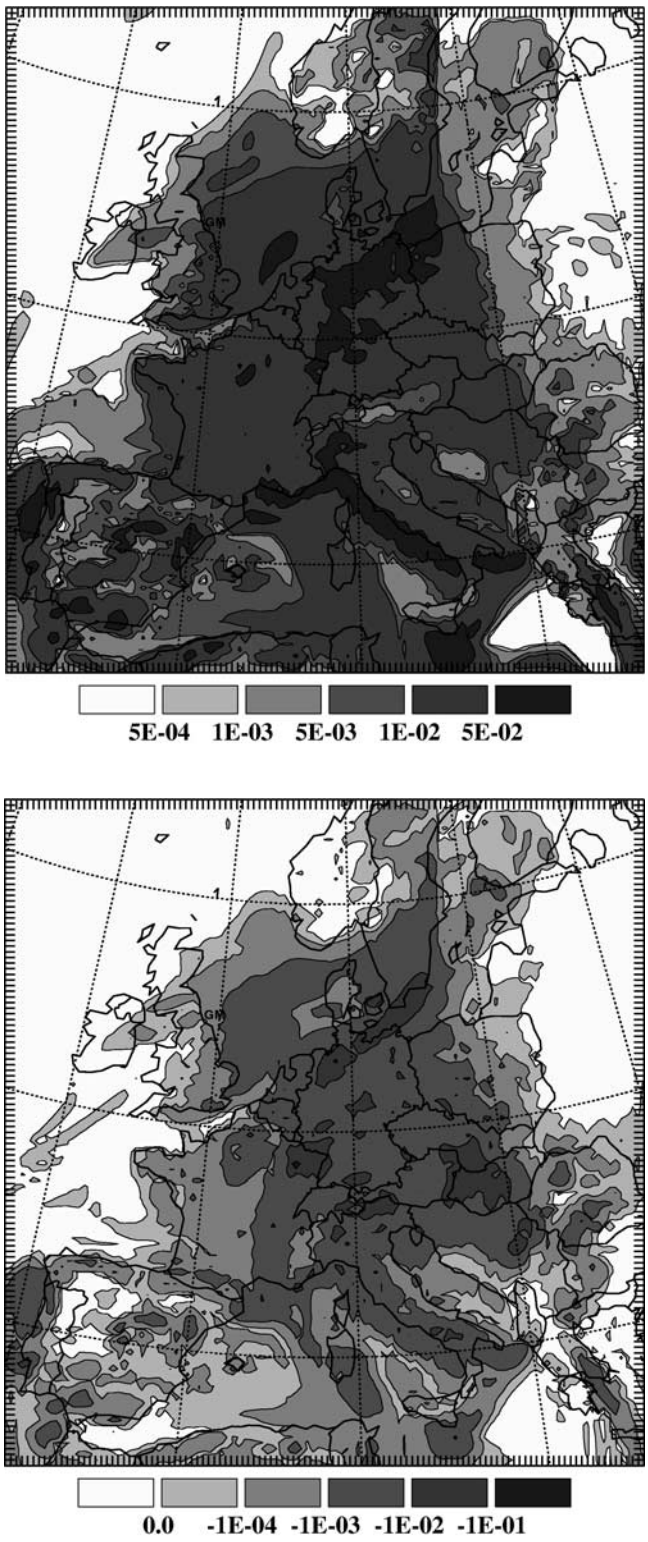

Figure 11b. Horizontal distribution of NO_3 (top) and ΔNO_3 (bottom) in ppb at 360 m above the surface at 0000 UTC for the EURAD/MADE simulation.

Figure 9 shows the horizontal distributions of emissions of SO_2, NO_x, anthropogenic VOC and NH_3 of a typical workday in tonnes per day. Biogenic emissions of isoprene and monoterpenes are calculated online using the parameterization provided by *Lübkert and Schöpp* [1989]. Particle emissions are based on the anthropogenic particulate matter emission inventory of 1993 compiled by TNO [*TNO*, 1997]. This inventory provides annual national total mass emissions on the European scale for two size classes, PM10 and PM2.5, and 10 source categories. The inven-

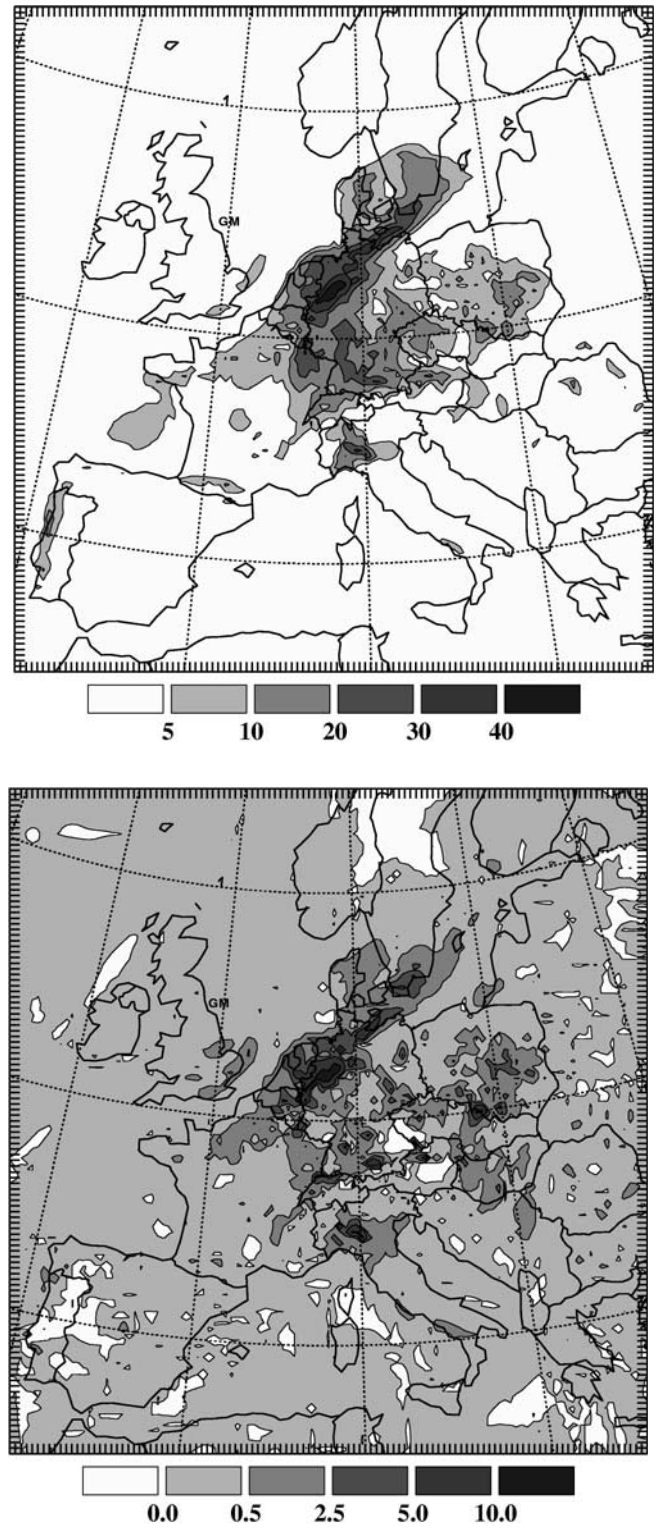

Figure 11c. Horizontal distribution of NO_3^- (top) and ΔNO_3^- (bottom) in ppb close to the surface at 0000 UTC for the EURAD/MADE simulation.

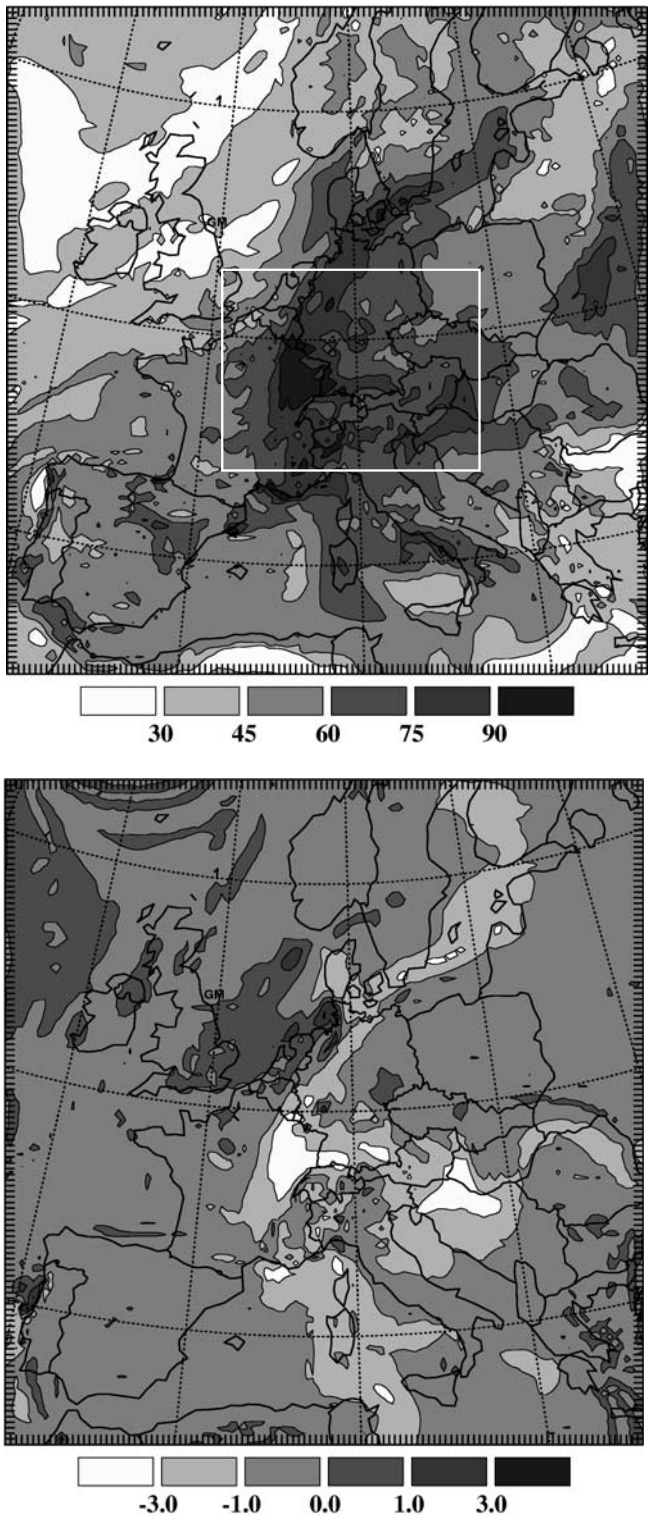

Figure 11d. Horizontal distribution of O_3 (top) and ΔO_3 (bottom) in ppb close to the surface at 1300 UTC for the EURAD/MADE simulation.

tory available provides emission data with a horizontal resolution of 0.25° × 0.5°. Based on this inventory particle emissions are calculated for elemental carbon, primary organics, and anthropogenic primary PM2.5 for the fine modes, as well as emissions of anthropogenic coarse mode particles on the required temporal and spatial resolution.

5.2.3. EURAD/MADE Results

[59] Figure 10 shows the horizontal distribution of the geopotential, temperature and wind at 850 hPa on 7 July 1995, 0000 UTC. A high pressure system with low wind speed is located in the center of the model domain. Lows are centered over the Adriatic Sea and in East of Iceland. Strong westerly to southwesterly winds are found in the northern part of the model domain, northeasterly to northern winds are found over the western Mediterranean.

[60] Similar to the procedure described in section 5.1.3, two model runs were carried out to quantify the effects of the heterogeneous hydrolysis of N_2O_5 on the concentrations of individual air constituents and on the chemical composition of fine particles. For the reference case heterogeneous hydrolysis, including the nitrate effect, is taken into account, whereas for the sensitivity run heterogeneous hydrolysis of N_2O_5 is neglected.

[61] In the following we present the results for the selected species for the simulation with heterogeneous hydrolysis and the concentration difference between this simulation and the simulation without heterogeneous hydrolysis. Again, horizontal distributions are shown at those heights and points of time at which the maximum concentrations for the individual species are reached.

[62] Figure 11a shows the horizontal distributions of N_2O_5 (top) and the aerosol surface area density (bottom) for the reference case at 0000 UTC at approximately 130 m above the surface. The highest concentrations of N_2O_5 are found in the central part of the model domain along the west coast of Italy and along the west coast of Portugal. The maximum concentrations are on the order of 1 ppb, which is similar to the concentration levels we found for the KAMM/DRAIS results. The maximum surface area densities are on the order of 1500 μm^2 cm^{-3} and are therefore about three times higher than those we found for the situation described in section 5.1.3. This difference is caused by the almost stagnant conditions in the southwestern part of Germany and the contributions of secondary organic and primary particle compounds. The high surface area densities over the western Mediterranean is due to transport of polluted air masses through the Rhone valley by the northerly flow in that area.

[63] Figure 11b shows the horizontal distributions of NO_3 (top) and the difference of the simulations with and without heterogeneous hydrolysis (ΔNO_3, bottom) at 360 m above the surface at 0000 UTC. If hydrolysis is taken into account NO_3 concentrations are significantly lower than the values of the KAMM/DRAIS simulations (section 5.1.3) The reason for this is the much higher surface area density in the EURAD/MADE case. If heterogeneous hydrolysis is not considered, the results of KAMM/DRAIS and EURAD/MADE show comparable concentration levels of NO_3.

[64] Due to the high nitrate content of the aerosol exceeding 40 $\mu g\ m^{-3}$ (Figure 11c, top), the surface area densities reach high values as shown in Figure 11a. If heterogeneous hydrolysis is not considered the nitrate content of the aerosol is reduced by up to 10 $\mu g\ m^{-3}$.

[65] Finally, we consider the impact of the heterogeneous hydrolysis on the ozone concentration. Figure 11d gives the horizontal distribution of ozone and ΔO_3 close to the

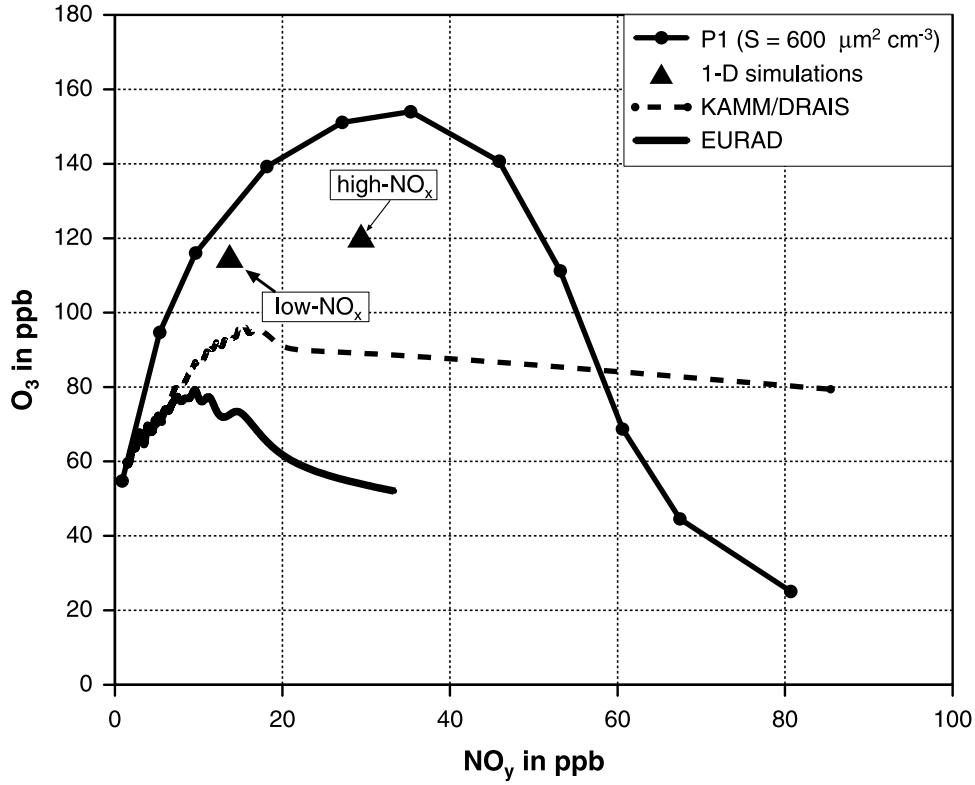

Figure 12. O_3 versus NO_y for the individual model runs using parameterization P1 (box-model runs) and P1* in case of the 1-D and 3-D simulations. For details see text.

surface at 1300 UTC. The ozone concentration varies from 30 ppb in very remote areas up to 100 ppb in the center of the model domain. In most parts of the model domain, ozone values decrease when the hydrolysis is taken into account, but also areas with increasing values can be found. In the area, which is covered both by the KAMM/DRAIS simulation and the EURAD/MADE simulation a reduction of ozone is found when the hydrolysis of N_2O_5 is taken into account, which is consistent with the KAMM/DRAIS results. However, the overall changes of ozone caused by heterogeneous hydrolysis of N_2O_5 are small (on the order of 5%).

6. Photochemical Conditions of Individual Simulations

[66] Figure 12 contrasts the photochemical conditions of the individual simulations. Analogous to Figure 2 the O_3 concentration versus the NO_y concentration is shown. The highest values for both O_3 and NO_y are reached by the box model simulations because in this case neither deposition nor transport processes are included. The 1-D simulations are represented by two data points taken at 17 m above surface, one for the low-NO_x case the other for the high-NO_x case. Here deposition and vertical diffusion are included which leads to lower concentration levels of NO_y and O_3.

[67] In order to present the data of the 3-D simulations in a similar way we applied a smoothing procedure described in *Vogel et al.* [1999] to the entire simulated data at 1400 CET at 20 m above surface for the situations depicted in Figures 8d and 11d. For the EURAD simulations we used the data inside the rectangular depicted in Figure 11d only. While the maximum mean ozone concentration of the KAMM/DRAIS simulations reaches 96 ppb at a mean NO_y concentration of 16 ppb these values are both lower for the EURAD simulations. This demonstrates that very different conditions have been evaluated. Our simulations covered slightly polluted and highly polluted conditions as well as low-NO_x conditions and high-NO_x conditions.

7. Conclusions

[68] We quantified the impact of heterogeneous hydrolysis of N_2O_5 on tropospheric chemistry and on nitrate aerosol formation by using recent findings on the heterogeneous reaction probability of N_2O_5 derived from laboratory measurements performing model simulations with the comprehensive model systems KAMM/DRAIS and EURAD/MADE. The model systems have been applied to the southwestern part of Germany and Central Europe, respectively. As a starting point pure chemistry box model runs were carried out neglecting transport and deposition processes. For the box model runs the surface area density was prescribed and kept constant with time. These investigations have shown that the heterogeneous hydrolysis of N_2O_5 leads to a decrease of ozone under low-NO_x conditions and to a strong increase of ozone under high-NO_x conditions. We showed that a simple parameterization of the hydrolysis of N_2O_5 that was commonly used in 3-D air quality models overestimates the effect of heterogeneous hydrolysis on photochemistry.

[69] Simulations with the one-dimensional version of KAMM/DRAIS, which takes into account vertical mixing processes and deposition, the temporal changes of the emissions and secondary inorganic aerosol have shown that the effect of the heterogeneous hydrolysis of N_2O_5 on ozone decreases considerably compared to the box model simulations. This is caused by vertical mixing processes and by the differing locations of the maximum aerosol surface area density and the maximum N_2O_5 concentration. However, a large impact of the heterogeneous hydrolysis of N_2O_5 was found on the nocturnal concentrations of N_2O_5, NO_3, HNO_3, the aerosol surface area density and the nitrate content of the aerosol. We also studied the impact of the so-called nitrate effect, which means that the presence of nitrate in the aerosol lowers the reaction probability of the hydrolysis by one order of magnitude. This effect becomes important especially under high-NO_x conditions.

[70] Finally, simulations with the three-dimensional versions of KAMM/DRAIS and EURAD/MADE were carried out. The results of those simulations, which are the most realistic confirmed the findings of the 1-D simulations.

[71] Overall, we conclude that the detailed surface area dependent treatment of heterogeneous N_2O_5 hydrolysis should be taken into account in chemistry transport models. Although its impact on ozone is small, it causes remarkable changes in the nocturnal concentrations of nitrogen containing species and on aerosol properties such as surface area density and nitrate content.

[72] **Acknowledgments.** We acknowledge the valuable comments of the anonymous reviewers. We thank Thomas Mentel who gave us fast access to his data and who discussed with us several aspects of the paper.

References

Ackermann, I. J., H. Hass, M. Memmesheimer, A. Ebel, F. S. Binkowski, and U. Shankar, Modal aerosol dynamics model for Europe: Development and first applications, *Atmos. Environ.*, *32*, 2981–2999, 1998.

Adrian, G., and F. Fiedler, Simulation of unstationary wind and temperature fields over complex terrain and comparison with observations, *Contr. Atmos. Phys.*, *64*, 27–48, 1991.

Baer, M., and K. Nester, Parameterization of trace gas dry deposition velocities for a regional mesoscale diffusion model, *Ann. Geophysicae*, *10*, 912–923, 1993.

Behnke, W., C. George, V. Scheer, and C. Zetsch, Production and decay of $ClNO_2$ from the reaction of gaseous N_2O_5 with NaCl solution: Bulk and aerosol experiments, *J. Geophys. Res.*, *102*, 3795–3804, 1997.

Binkowski, F. S., Aerosols in MODELS-3 CMAQ, in *Science Algorithms of the EPA Models-3 Community Air Quality* (*CMAQ*) *Modeling System*, EPA 600/R-99-030, http:/www.epa.gov/asmdnerl/models3, 1999.

Binkowski, F. S., and U. Shankar, The regional particulate matter model, 1, Model description and preliminary results, *J. Geophys. Res.*, *100*, 1729–1736, 1995.

Chang, J. S., R. A. Brost, I. S. A. Isaksen, S. Madronich, P. Middleton, W. R. Stockwell, and C. J. Walcek, A three-dimensional Eulerian acid deposition model: Physical concepts and formulation, *J. Geophys. Res.*, *92*, 14,681–14,700, 1987.

Corsmeier, U., et al., Ozone and PAN formation inside and outside of the Berlin plume – Process analysis and numerical process simulation, *J. Atm. Chem.*, *42*, 289–322, 2002.

Dentener, F. J., and P. J. Crutzen, Reaction of N_2O_5 on tropospheric aerosols: Impact on the global distributions of NO_x, O_3, and OH, *J. Geophys. Res.*, *98*, 7149–7163, 1993.

Derwent, R. G., and M. E. Jenkin, Hydrocarbons and the long-range transport of ozone and PAN across Europe, *Atmos. Environ.*, *25*, 1661–1678, 1991.

Ebel, A., H. Elbern, H. Hass, H. J. Jakobs, M. Memmesheimer, M. Laube, A. Oberreuter, and G. Piekorz, Simulation of chemical transformation and transport of air pollutants with the model system EURAD, in *Transport and Chemical Transformation of Pollutants in the Troposphere*, vol. 7, edited by P. Borell et al., pp. 27–45, Springer-Verlag, New York, 1997.

Ehhalt, D. H., and J. W. Drummond, The tropospheric cycle of NO_x, in *Chemistry of the Unpolluted and Polluted Troposphere*, edited by H. Georgii and W. Jaeschke, pp. 219–251, D. Reidel, Norwell, Mass., 1982.

EMEP, *MSC-W Status Report 1998 – Part 1*, MSC-W, Norwegian Meteorol. Inst., Oslo, Norway, 1998.

European Commission, *Auto-Oil II Programme, Final Report*, DG Environment, Brussels, Belgium, 2000.

Fenter, F. F., F. Caloz, and M. J. Rossi, The heterogeneous kinetics of N_2O_5 uptake on salt, with a systematic study of the role of surface presentation (for N_2O_5 and HNO_3), *J. Phys. Chem.*, *100*, 1008–1019, 1996.

Fiedler, F., I. Bischoff-Gauß, N. Kalthoff, and G. Adrian, Modeling of transport and diffusion of a tracer in the Freiburg-Schauinsland area, *J. Geophys. Res.*, *105*, 1599–1610, 2000.

Fuchs, N. A., and A. G. Sutugin, High-dispersed aerosols, in *International Reviews of Aerosol Physics and Chemistry*, vol. 2, edited by G. M. Hidy and J. R. Brock, Pergamon, New York, 1971.

Geyer, A., B. Alicke, S. Konrad, T. Schmitz, J. Stutz, and U. Platt, Chemistry and oxidation capacity of the nitrate radical in the continental boundary layer near Berlin, *J. Geophys. Res.*, *106*, 8013–8026, 2001.

Geyer, A., A. Hofzumahaus, F. Holland, S. Konrad, T. Klüpfel, H.-W. Pätz, D. Perner, H.-J. Schäfer, A. Volz-Thomas, and U. Platt, Nighttime production of peroxy and hydroxyl radicals during the BERLIOZ campaign: Observations and modeling studies, *J. Geophys. Res.*, *108*, 8249, doi:10.1029/2001JD000656, 2003.

Grell, G. A., J. Dudhia, and D. R. Stauffer, A description of the fifth-generation Penn State/NCAR mesoscale model (MM5), *Technical Note TN-398+STR*, Natl. Cent. Atmos. Res., Boulder, Colo., 1994.

Hallquist, M., D. J. Stewart, J. Baker, and R. A. Cox, Hydrolysis of N_2O_5 on submicron sulfuric acid aerosols, *J. Phys. Chem.*, *104*, 3984–3990, 2000.

Hammer, M.-U., B. Vogel, and H. Vogel, Findings on H_2O_2/HNO_3 as an indicator of ozone sensitivity in Baden-Württemberg, Berlin-Brandenburg, and the Po Valley based on numerical simulations, *J. Geophys. Res.*, *107*, doi:10.1029/2000JD000211, 2002.

Hass, H., H. J. Jakobs, and M. Memmesheimer, Analysis of a regional model (EURAD) near surface gas concentration predictions using observations from networks, *Meteorol. Atmos. Phys.*, *57*, 173–200, 1995.

Hendricks, J., Modellstudien zur Bedeutung heterogener Reaktionen auf und in Sulfataerosolen für die Photochemie der Tropopausenregion mittlerer Breiten, *Mitteilungen aus dem Institut für Geophysik und Meteorologie der Universität zu Köln*, Heft 122, Köln, 1997.

Hu, J. H., and J. P. D. Abbatt, Reaction probabilities for N_2O_5 hydrolysis on sulfuric acid and ammonium sulfate aerosols at room temperature, *J. Phys. Chem.*, *101*, 871–878, 1997.

Kuhn, M., et al., Intercomparison of the gas phase chemistry in several chemistry and transport models, *Atmos. Environ.*, *32*, 693–709, 1998.

Lamb, B., A. Guenther, D. Gay, and H. Westberg, A national inventory of biogenic hydrocarbon emissions, *Atmos. Environ.*, *21*, 1695–1705, 1987.

Logan, J., Nitrogen oxides in the troposphere: Global and regional budgets, *J. Geophys. Res.*, *88*, 10,785–10,807, 1983.

Lübkert, B., and W. Schöpp, A model to calculate natural VOC emissions from forests in Europe, *IIASA working paper WP-89-082*, IIASA, Laxenburg, Austria, 1989.

Ludwig, J., F. X. Meixner, B. Vogel, and J. Förstner, Soil-air exchange of nitric oxide: An overview of processes, environmental factors, and modeling studies, *Biogeochemistry*, *52*, 225–258, 2001.

McKeen, S. A., E.-Y. Hsie, and S. C. Liu, A study of the dependence of rural ozone on ozone precursors in the eastern United States, *J. Geophys. Res.*, *96*, 15,377–15,394, 1991.

Memmesheimer, M., H. Hass, J. Tippke, and A. Ebel, Modeling of episodic emission data for Europe with the EURAD emission model EEM, in *Proceedings of the International Speciality Conference 'Regional Photochemical Measurement and modeling studies'*, vol. 2, edited by A. Ranzieri and P. Solomon, pp. 495–499, AWMA, San Diego, Calif., 1995.

Mentel, T. F., M. Sohn, and A. Wahner, Nitrate effect in the heterogeneous hydrolysis of dinitrogen pentoxide on aqueous aerosols, *Phys. Chem. Chem. Phys.*, *1*, 5451–5457, 1999.

Mihelcic, D., D. Klemp, P. Müsgen, H. W. Pätz, and A. Volz-Thomas, Simultaneous measurements of peroxy and nitrate radicals at Schauinsland, *J. Atmos. Chem.*, *16*, 313–335, 1993.

Mozurkewich, M., and J. G. Calvert, Reaction probabilities of N_2O_5 on aqueous aerosols, *J. Geophys. Res.*, *93*, 15,889–15,896, 1988.

Nester, K., H.-J. Panitz, and F. Fiedler, Comparison of the DRAIS an EURAD model simulations of air pollution in a mesoscale area, *Meteorol. Atmos. Phys.*, *57*, 135–158, 1995.

Obermeier, A., R. Friedrich, C. John, J. Seier, H. Vogel, F. Fiedler, and B. Vogel, Photosmog: Möglichkeiten und Strategien zur Verminderung des bodennahen Ozons, *Umweltforschung in Baden-Württemberg*, ecomed Verlagsgesellschaft, Landsberg, 1995.

Platt, U. F., A. M. Winer, H. W. Biermann, R. Atkinson, and J. N. Pitts Jr., Measurement of nitrate radical concentrations in continental air, *Environ. Sci. Technol.*, *18*, 365–369, 1984.

Platt, U. F., G. Le Bras, G. Poulet, J. P. Burrows, and G. K. Moortgat, Peroxy radicals from nighttime reaction of NO_3 with organic compounds, *Nature*, *348*, 147–149, 1990.

Pregger, T., R. Friedrich, A. Obermeier, B. Wickert, P. Blank, J. Theloke, H. Vogel, N. Riemer, B. Vogel, and F. Fiedler, Entwicklung von Instrumenten zur Analyse der Umweltbelastungen durch Feinstäube und andere ausgewählte Luftverunreinigungen in Baden-Württemberg, http://bwplus.fzk.de, 1999.

Robinson, G. N., D. R. Worsnop, J. T. Jayne, and C. E. Kolb, Heterogeneous uptake of $ClONO_2$ and N_2O_5 by sulfuric acid solutions, *J. Geophys. Res.*, *102*, 3583–3601, 1997.

Ruggaber, A., R. Dlugi, and T. Nakajiima, Modelling radiation quantities and photolysis frequencies in the troposphere, *J. Atmos. Chem.*, *18*, 171–210, 1994.

Schädler, G., Triggering of atmospheric circulations by moisture inhomogeneities of the Earth's surface, *Bound. Layer Meteorol.*, *51*, 1–29, 1989.

Schell, B., I. J. Ackermann, H. Hass, F. S. Binkowski, and A. Ebel, Modeling the formation of secondary organic aerosol within a comprehensive air quality model system, *J. Geophys. Res.*, *106*, 28,275–28,293, 2001.

Seier, J., P. Berner, R. Friedrich, C. John, and A. Obermeier, Generation of an emission data base for TRACT, in *Exchange and Transport of Air Pollutants over Complex Terrain and the Sea*, edited by S. Larsen, F. Fiedler, and P. Borrell, pp. 269–278, Springer-Verlag, New York, 2000.

Stockwell, W. R., and D. Kley, The Euro-RADM mechanism: A gas-phase mechanism for European air quality studies, *Berichte des Forschungszentrums Jülich, 2868,*Jülich, Germany, 1994.

Stockwell, W. R., P. Middleton, and J. S. Chang, The second generation regional acid deposition model chemical mechanism for regional air quality modeling, *J. Geophys. Res.*, *95*, 16,343–16,367, 1990.

Stockwell, W. R., F. Kirchner, M. Kuhn, and S. Seefeld, A new mechanism for regional atmospheric chemistry modeling, *J. Geophys. Res.*, *102*, 25,847–25,879, 1997.

TNO, Particulate Matter Emissions (PM10, PM2.5, PM<0.1) in Europe in 1990 and 1993, TNO Report TNO-MEP-R96/472, Netherlands, 1997.

Van Doren, J. M., L. R. Watson, P. Davidovits, D. R. Worsnop, M. S. Zahniser, and C. E. Kolb, Temperature dependence of the uptake coefficients of HNO_3, HCl, and N_2O_5 by water droplets, *J. Phys. Chem.*, *94*, 3265–3269, 1990.

Vogel, B., F. Fiedler, and H. Vogel, Influence of topography and biogenic volatile organic compounds emission in the state of Baden-Wuerttemberg on ozone concentrations during episodes of high air temperatures, *J. Geophys. Res.*, *100*, 22,907–22,928, 1995.

Vogel, B., N. Riemer, H. Vogel, and F. Fiedler, Findings on NO_y as an indicator for ozone sensitivity based on different numerical simulations, *J. Geophys. Res.*, *104*, 3605–3620, 1999.

von Friedeburg, C., T. Wagner, A. Geyer, N. Kaiser, B. Vogel, H. Vogel, and U. Platt, Derivation of tropospheric NO_3 profiles using off-axis-DOAS measurements during sunrise and comparison with simulations, *J. Geophys. Res.*, *107*, 4168, doi:10.1029/2001JD000481, 2002.

Wahner, A., T. Mentel, M. Sohn, and J. Stier, Heterogeneous reaction of N_2O_5 on sodium aerosol, *J. Geophys. Res.*, *103*, 31,103–31,112, 1998.

Wickert, B., U. Schwarz, P. Blank, C. John, J. Kühlwein, A. Obermeier, R. Friedrich, Generation of an emission data base for Europe 1994, in *Proceedings of EUROTRAC Symposium '98*, vol. 2, edited by P. M. Borrell and P. Borrell, pp. 255–260, WITPress, Boston, Southampton, 1999.

Yienger, J. J., and H. Levy II, Empirical model of global soil-biogenic NO_x emissions, *J. Geophys. Res.*, *100*, 11,447–11,464, 1995.

Zimmermann, J., and D. Poppe, A supplement for the RADM2 chemical mechanism: Photooxidation of isoprene, *Atmos. Environ.*, *30*, 1255–1269, 1996.

N. Riemer, B. Vogel, and H. Vogel, Institut für Meteorologie und Klimaforschung, Forschungszentrum Karlsruhe/Universität Karlsruhe, Postfach 3640, 76021 Karlsruhe, Germany. (nsriemer@ucdavis.edu; bernhard.vogel@imk.fzk.de; heike.vogel@imk.fzk.de)

I. Ackermann, H. Hass, C. Kessler, and B. Schell, Ford Forschungszentrum Aachen, Süsterfeldstraße 200, 52072,Aachen, Germany. (iackerma@ford.com; hhass@ford.com; ckessle2@ford.com; bschell@ford.com)